

## Thermoelectric and thermal transport properties of complex oxide thin films, heterostructures and superlattices

Jayakanth Ravichandran<sup>a)</sup>

Mork Family Department of Chemical Engineering and Materials Science, University of Southern California, Los Angeles, CA 90089, USA

(Received 25 June 2016; accepted 24 October 2016)

Over the years, the search for high performance thermoelectric materials has been dictated by the “phonon glass and electron crystal (PGEC)” paradigm, which suggests that low band gap semiconductors with high atomic number elements and high carrier mobility are the ideal materials to achieve high thermoelectric figure of merit. Complex oxides provide alternative mechanisms such as large density of states and strong electron correlation for high thermoelectric efficiency, albeit having low carrier mobility. Due to vast structural and chemical flexibility, they provide a fertile playground to design high efficiency thermoelectric materials. Further, developments in oxide thin film growth methods have enabled synthesis of high quality, atomically precise low dimensional structures such as heterostructures and superlattices. These materials and structures act as excellent model systems to explore nanoscale thermal and thermoelectric transport, which will not only expand the frontier of our knowledge, but also continue to enable cutting edge applications.



Jayakanth Ravichandran

Jayakanth Ravichandran is currently an Assistant Professor in the Mork Family Department of Chemical Engineering and Materials Science, University of Southern California. He received his B.Tech, and M.Tech in Metallurgical and Materials Engineering from Indian Institute of Technology, Kharagpur, India in 2007, and completed his Ph.D. in Applied Science and Technology from University of California, Berkeley in 2011. He was a post-doctoral fellow at Columbia University (2012–2014) and Harvard University (2014) before his current appointment. Currently, his research group’s interests include design, synthesis, characterization, and transport properties of complex ionic materials, and thin film science and technology. Often, the materials investigated in his group have relevance to electronic, photonic and energy applications.

### I. INTRODUCTION

Thermoelectricity is a process of direct inter-conversion of thermal and electrical energy using a solid-state engine. The efficiency of a thermoelectric engine is related to a material dependent figure of merit,  $ZT$  and the Carnot efficiency.  $Z$  is given as  $\alpha^2\sigma/\kappa$ , where  $\alpha$  is Seebeck coefficient or thermopower,  $\alpha^2\sigma$  is power factor, and  $\sigma$  and  $\kappa$  are electrical and thermal conductivity respectively.<sup>1</sup> Due to conflicting inter-relationships between these three parameters, every material has an optimal  $Z$ , and significant fraction of research on thermoelectrics has been focused on identifying high efficiency thermoelectric materials and optimizing their  $ZT$ .<sup>1,2</sup> The two key

methods for optimizing  $Z$  are reduction of lattice or phonon thermal conductivity without affecting the electrical properties,<sup>3</sup> and tuning the carrier concentration (very rarely band structure) by doping or alloying.<sup>4</sup> While a thermoelectric engine possesses several advantages over other waste heat recovery technologies, such as lack of moving parts, reliability etc., low efficiency of thermoelectric engines have limited their application for waste heat recovery.<sup>1</sup>

Although optimization of thermoelectric properties of known semiconductors have been successful in achieving high  $Z$ , further improvements in  $Z$  and expanding the operating temperature range of thermoelectric engine requires renewed materials discovery efforts.<sup>2,5</sup> One of the paradigms that had dictated the search for high efficiency thermoelectric materials has been the “phonon glass and electron crystal (PGEC)” paradigm proposed by Slack.<sup>6</sup> Several new materials showing high thermoelectric efficiency were discovered

Contributing Editor: Terry M. Tritt

<sup>a)</sup>Address all correspondence to this author.

e-mail: jayakanr@usc.edu

DOI: 10.1557/jmr.2016.419

with this mechanism as the basis.<sup>7–9</sup> Later, the prediction of high thermoelectric efficiency in low dimensional materials by Dresselhaus<sup>10,11</sup> led to experimental realization of several high efficiency nanostructured thermoelectric materials.<sup>12–15</sup> An extensive review of nanostructured thermoelectric materials can be found elsewhere.<sup>16</sup> Most of the materials discussed above are semiconductors, which are composed of heavy elements that are either toxic or not earth abundant. This limits the large scale sustainable deployment of thermoelectric materials, even if they have high efficiency.<sup>17–19</sup>

Recently, the discovery of high thermoelectric efficiency in n-type SrTiO<sub>3</sub> (Ref. 20) and Na<sub>x</sub>CoO<sub>2</sub> (Ref. 21) generated significant interest in oxide thermoelectrics. These discoveries were unexpected, as oxides have defied most of the materials descriptors necessary to achieve high thermoelectric efficiency.<sup>1</sup> To understand the importance of these discoveries, we must first address the origin of the differences between electronic transport properties of complex oxides and conventional thermoelectric semiconductors such as Bi<sub>2</sub>Te<sub>3</sub>, PbTe etc. The conduction and valence band of d-band complex oxides are often *d*-orbital and *d*-orbital/*p*-orbital character, respectively (although some complex oxides can possess *s*-orbital and *p*-orbital character), whereas conventional semiconductors are often *s*-orbital and *p*-orbital character, respectively. Materials containing *s*-orbital and *p*-orbital character often tend to be more dispersive, and hence, possess small effective mass, large bandwidth, and high carrier mobility. On the other hand, the small bandwidth and large density of states in d-band complex oxides are a consequence of *d*-orbital character, which leads to large effective mass and low carrier mobility. The ionic nature of oxides leads to strong electron–phonon coupling, and hence, small electron relaxation time. However, large density of states and high effective mass leads to large thermopower in these oxides even at very high filling.<sup>22</sup> The same factors such as electron interaction and magnetism that leads to low carrier mobility in oxides often result in high thermopower.<sup>23,24</sup> These insights also signaled the discovery of possibly new mechanisms toward high thermoelectric efficiency. Although the full potential of these new mechanisms are yet to be fully realized, they make complex oxides one of the most competitive thermoelectric materials system, especially for high temperature applications.

Complex oxides provide a wide range of chemical and structural flexibility to discover high efficiency thermoelectric materials. On the microscopic level, electrons in complex oxides are affected by the interplay between spin, orbital, lattice, and charge degrees of freedom, all of which have profound effects on the thermoelectric properties and offer a completely new approach to thermoelectric research. Additionally, complex oxides are often composed of earth abundant elements, which

are inexpensive and environmentally friendly. Thus, they present both scientifically and technologically attractive features for thermoelectric research. These aspects are summarized in Fig. 1. Thin film oxide thermoelectrics provide researchers an efficient platform to access high quality materials (comparable to bulk single crystals) to understand their fundamental transport properties, as bulk single crystal growths are often time consuming and cumbersome. Moreover, with the growing necessity for on-chip cooling in several electronic and photonic technologies,<sup>25</sup> active temperature control in thermochemistry-on-a-chip, DNA microarrays, fiber-optic switches, micro-electro-mechanical systems,<sup>13</sup> and miniaturized, autonomous, and reliable power generators, and sensors in internet of things (IoT) type applications,<sup>26</sup> thin film thermoelectrics are expected to have an increasing role in applications beyond waste heat recovery and simple cooling applications.

Several reviews have already addressed the importance of oxide thermoelectrics and some of the salient materials families have been explored in detail.<sup>27–34</sup> Despite growing interest in thin film oxide thermoelectrics, as far as I am aware of, only one study surveys thermoelectric studies on thin films materials in depth, but was limited to two materials systems namely ZnO and Ca<sub>3</sub>Co<sub>4</sub>O<sub>9</sub>.<sup>35</sup> The aim of this review is to bridge the gap in earlier reviews on studies related to low dimensional thermoelectric oxide materials and also, place an emphasis on discussing the physics behind achieving large thermoelectric figure of merit in these materials. Specifically, this review will discuss the recent developments in the study of thermoelectric and thermal transport behavior of complex oxides, synthesized in the form of thin films, heterostructures, and superlattices. As thermal transport in low dimensional materials is an interesting topic with close relevance to thermoelectric applications, special emphasis will be placed on thermal transport studies.

## II. MECHANISMS FOR HIGH THERMOELECTRIC EFFICIENCY

As noted earlier, besides the optimization of carrier concentration, two of the common mechanisms used to achieve high thermoelectric efficiency are: (i) reduction in thermal conductivity due to alloying, nanostructuring of materials, and composite formation,<sup>16,36–41</sup> and (ii) band engineering or tailoring the electronic structure to improve the power factor.<sup>42–44</sup> Often such techniques are commonly used for semiconductors to achieve high thermoelectric efficiency. In case of oxides, the mechanisms toward high thermoelectric efficiency are often different and varied in nature. We will first review the doping dependence of thermoelectric properties in conventional materials with a brief discussion on the physics

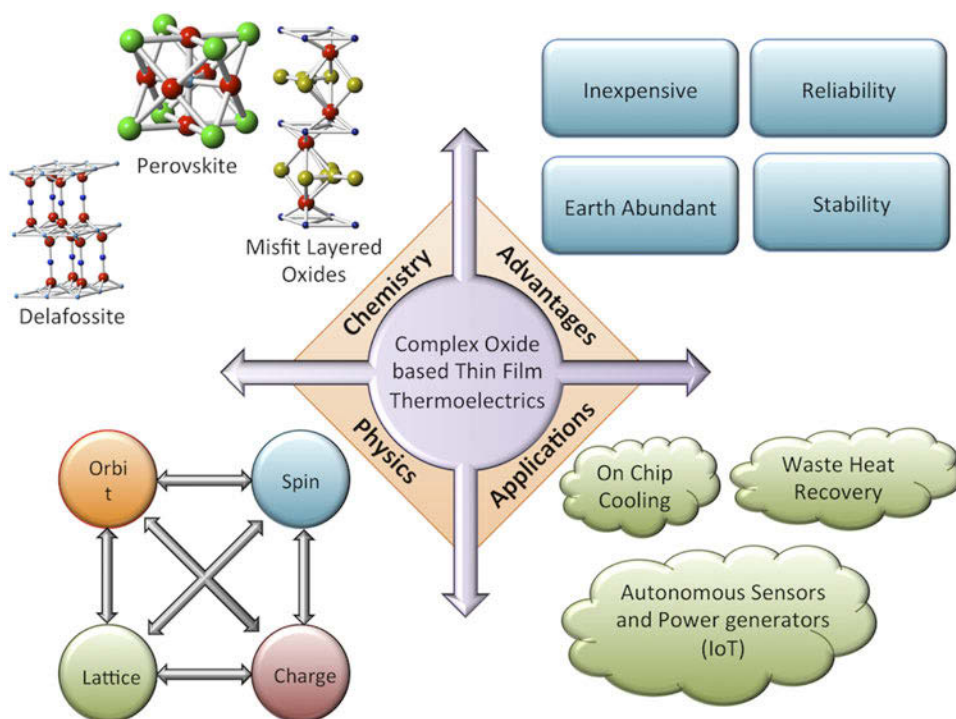


FIG. 1. A schematic showing the scientific and technological advantages of complex oxides as thermoelectrics: The bottom left shows how the interplay between different degrees of freedom (spin, charge, lattice, and orbit) enables new possibilities for complex oxide thermoelectrics; the top left shows the structural and chemical diversity, which affects the chemistry of complex oxides and their thermoelectric properties; the top right shows the advantages of complex oxides as materials system for any technological application; the bottom right shows the important applications, where complex oxide thermoelectrics, especially thin films can find an important role.

behind it, and discuss some of the new physical mechanisms that lead to high thermoelectric efficiency in complex oxides, to put them in context.

### A. Review of doping dependence of thermoelectric properties

The evolution of the thermoelectric properties as a function of carrier concentration (or equivalently chemical potential) is well understood for conventional materials irrespective of their electrical properties (insulating, semiconducting, semi-metallic, and metallic). These materials follow the conventional band picture of electron transport. Figure 2(a) motivates the physics behind how these properties are derived. Assuming the electron transport in the material is due to a single parabolic band, the density of states scales as square root of energy. Further, as electrons are Fermions, only a small bandwidth of energy ( $\sim$  few  $k_B T$ , where  $k_B$  is Boltzmann constant and  $T$  is temperature) close to the chemical potential is relevant for electron transport. As one shifts the chemical potential further into a band from an energy gap, the carrier concentration increases. As one can see, as the chemical potential increases and lies deeper into the band, the differential electrical conductivity (one should integrate the differential conductivity over the

whole energy range to obtain the electrical conductivity) increases, explaining why metals are good conductors compared to semiconductors. On the other hand, the first order moment of differential electrical conductivity is directly related to thermopower, hence, this value decreases as the chemical potential moves further deep into the band. This explains the origin of low thermopower of metals as compared to semiconducting materials. This conflicting nature of thermopower and electrical conductivity evolution with carrier concentration is the key reason why carrier concentration is used as an optimization parameter to achieve high  $Z$ . We show the conflicting nature of all the thermoelectric properties in Figs. 2(b) and 2(c) by plotting these properties as a function of carrier concentration, including thermal conductivity. As one can see, the electronic component of thermal conductivity can shift the optimal carrier concentration to achieve high  $ZT$  further from the optimum achieved for the power factor. Moreover, the phonon or lattice thermal conductivity has an important influence on the absolute value of  $ZT$  and not on the carrier concentration dependence. In the following discussion, we will review some of the novel mechanisms that enable high  $Z$  in oxide materials, to contrast the phenomenology discussed here for conventional semiconductor thermoelectric materials.

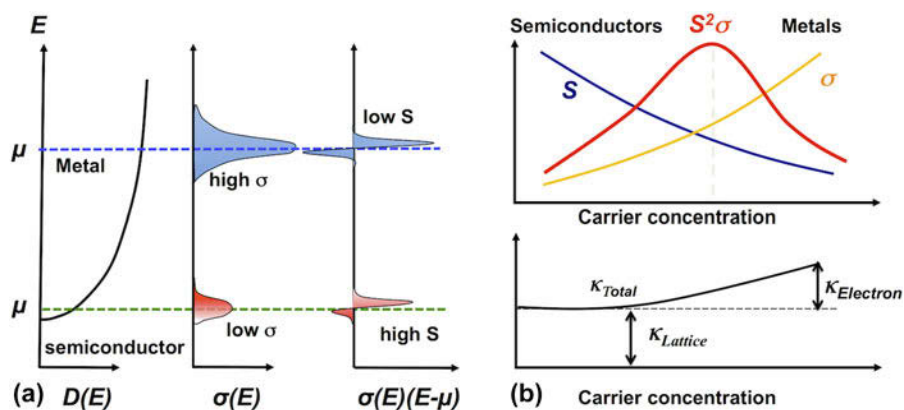


FIG. 2. Representation of thermoelectric parameters using band theory: (a) the evolution of density of states, differential electrical conductivity, and first order moment of differential electrical conductivity ( $x$ -axis) with energy. This schematic clearly distinguishes the thermoelectric properties of semiconductors and metals. (b) The dependence of thermoelectric properties on the carrier concentration. Neither semiconductors nor metals show high power factor due to too low conductivity and thermopower respectively, but the maximum occurs at intermediate carrier density, which corresponds to heavily doped (alloyed) semiconductors. The bottom panel shows that at high carrier density (metallic limit) the electronic thermal conductivity has an important contribution to the total thermal conductivity. This interplay between the three thermoelectric parameters (electrical and thermal conductivity, and thermopower) gives rise to an optimal carrier density, which shows maximum power factor.

## B. Orbital degeneracy in noninteracting or weakly interacting materials

It is well known that large degeneracy is desirable for increasing thermopower. Conventional high efficiency thermoelectric materials usually possess large valley degeneracy.<sup>1</sup> Transition metal oxides provide an alternate degeneracy mechanism namely orbital degeneracy. The conduction band of most thermoelectric transition metal oxides (especially perovskites) is dominated by the  $d$ -band character.<sup>45,46</sup> This  $d$ -band nature is the key reason for large orbital degeneracy in titanates, especially SrTiO<sub>3</sub> (STO). The transition metal  $d$ -orbitals possess the 5-fold degeneracy, when compared to one and three for  $s$ - and  $p$ -orbitals respectively. The nature of the degeneracy of transition metal oxides is sensitively dependent on the neighborhood of the transitional metal ions in the unit cell of the oxide. For example, STO crystallizes in the perovskite structure (CaTiO<sub>3</sub> type) and the nearest neighbor for the Ti<sup>4+</sup> ions are the O<sup>2-</sup>, which forms octahedra around the Ti<sup>4+</sup> ions. This octahedra leads to the crystal field splitting of the degenerate  $d$ -orbitals into 3-fold low energy  $t_{2g}$  orbitals and 2-fold high energy  $e_g$  orbitals.<sup>47-49</sup> The low-lying  $t_{2g}$  orbitals form the conduction band in STO. Besides, the small bandwidth of these bands lead to *high effective mass* in STO, which is considered desirable to achieve large thermopower, even if it adversely affects mobility.<sup>50</sup> This is one of the important consequences of the large orbital degeneracy, which enables high thermopower in STO even at very large dopant concentration such as  $10^{21}$  cm<sup>-3</sup>. Unfortunately, the low electron mobility of STO at room temperature (and higher temperatures) is largely due to strong electron-phonon coupling, which is the primary limitation for further increasing power

factor at room temperatures or higher.<sup>51-55</sup> Besides high effective mass, enhanced scattering rates of electrons (e.g., with phonons) is another reason for low mobility in such large density of states materials.

Okuda et al. achieved one of first experimental demonstrations of high thermoelectric power factor in complex oxides by systematically doping STO with La. They showed large thermoelectric power factor [ $\sim 36$   $\mu\text{W}/(\text{cm K}^2)$ ] in  $n$ -type doped STO at room temperature and established that large orbital degeneracy can lead to high power factor.<sup>20</sup> Such a large thermoelectric power factor is comparable to the state-of-the-art room temperature thermoelectric material, Bi<sub>2</sub>Te<sub>3</sub>.<sup>56</sup> Unfortunately, the larger thermal conductivity of STO [ $\sim 10$  W/(m K)] leads to a  $ZT$  of  $\sim 0.1$  at room temperature, as compared to Bi<sub>2</sub>Te<sub>3</sub>'s  $ZT$  of  $\sim 1-1.5$ .<sup>20,56</sup> Several strategies to improve the figure of merit by tailoring both the electrical and thermal properties are currently underway. Besides SrTiO<sub>3</sub>, other oxide materials such as doped SrNb<sub>2</sub>O<sub>6</sub>,<sup>34,57,58</sup> and Ba<sub>1-x</sub>Sr<sub>x</sub>PbO<sub>3</sub><sup>59,60</sup> that are being explored for potential high temperature applications.

## C. Orbital and spin degeneracy in strongly interacting materials

So far, we discussed electron transport in complex oxides, which can be explained by noninteracting or weakly interacting picture. In most complex oxides, this model fails, due to strong electron-electron correlation. Strong electron correlation (or electron-electron interaction) has been the subject of several interesting articles,<sup>61,62</sup> and we will provide a succinct summary of our current understanding of thermoelectric properties in strongly correlated systems. In a noninteracting or weakly interacting

picture, one can assume that the kinetic energy of the electrons is much greater than the periodic potential, which the electron experiences due to the presence of ionic lattice. In the strongly correlated regime, the on-site potential due to the lattice is much greater than the kinetic energy of the electrons, and hence, we need a completely different model to understand electronic transport. The electron transport, especially thermoelectric transport, in the strongly correlated regime has been a subject several theoretical investigations and provide a simple framework to explain all transport quantities.<sup>22,63–65</sup> This model, often called the single band Hubbard model, studies the evolution of various transport and physical properties for a strongly correlated system with on-site potential,  $U$  and hopping energy or bandwidth,  $t$  at a given temperature  $T$ . For a given site, to achieve a carrier occupation number other than 1, one has to pay an energy cost of  $U$  and the energy cost for a carrier hopping from one site to another is  $t$ . For a strongly correlated system,  $U \gg t$ . The thermoelectric transport quantities such as electrical conductivity, thermopower, and electronic component of thermal conductivity etc. can be derived as analytical expressions.<sup>22</sup> The results from such a model can elucidate the evolution of power factor ( $TS^2\sigma$  shown in y-axis) as a function of  $\rho$  or filling (average electron or carrier occupation on a site shown in x-axis) in  $\text{Na}_x\text{CoO}_2$ , which is one of the important correlated thermoelectric oxide [shown in Fig. 3(a)]. Many correlated perovskite oxides such as manganites [especially  $\text{CaMnO}_3$  (Ref. 66–68)], chromates,<sup>69</sup> ruthanates,<sup>70</sup> and cobaltates<sup>21,71–73</sup>

show promising thermoelectric properties and largely follow this formalism.

Among these compounds, cobaltates show very high figure merit over a wide temperature range,<sup>71,73</sup> and is considered one of the most important high temperature thermoelectric systems, especially for p-type oxides.<sup>74,75</sup> The large thermoelectric power factor observed in cobaltates is explained using spin degeneracy.<sup>23,24</sup> Later, this hypothesis was verified experimentally using in depth transport studies.<sup>76</sup> For cobaltates, the valence state ranges from +3 to +4 with 6 and 5 electrons to be filled in the d-bands. Ideally, one would expect the low spin state ( $t_{2g}^6$  for  $\text{Co}^{3+}$  and  $t_{2g}^5$  for  $\text{Co}^{4+}$ ) to be stable, but the competition between the crystal field splitting energy and the Hund's rule coupling (intra-atomic exchange) can help us access states with larger degeneracy, which is often dubbed as *spin degeneracy*. This competition is also responsible for partially filled  $t_{2g}$  and  $e_g$  orbitals, and degenerate spin states in cobaltates (low spin:  $t_{2g}^6$  for  $\text{Co}^{3+}$  and  $t_{2g}^5$  for  $\text{Co}^{4+}$ , intermediate spin:  $t_{2g}^5e_g^1$  for  $\text{Co}^{3+}$  and  $t_{2g}^4e_g^1$  for  $\text{Co}^{4+}$  and high spin:  $t_{2g}^4e_g^2$  for  $\text{Co}^{3+}$  and  $t_{2g}^3e_g^2$  for  $\text{Co}^{4+}$ ). This spin degeneracy, on top of the orbital degeneracy possible in these systems, gives rise to large thermoelectric power in cobaltates [the electronic structures and the degeneracies are schematically shown in Fig. 3(b)]. The combined effect of spin and orbital degeneracy leads to large thermopower only in triangularly coordinated cobalt lattices as seen in  $\text{Na}_x\text{CoO}_2$ , where the bond angle for Co–O–Co bonds is  $90^\circ$ .<sup>24</sup> This framework can also be used to understand the thermally induced

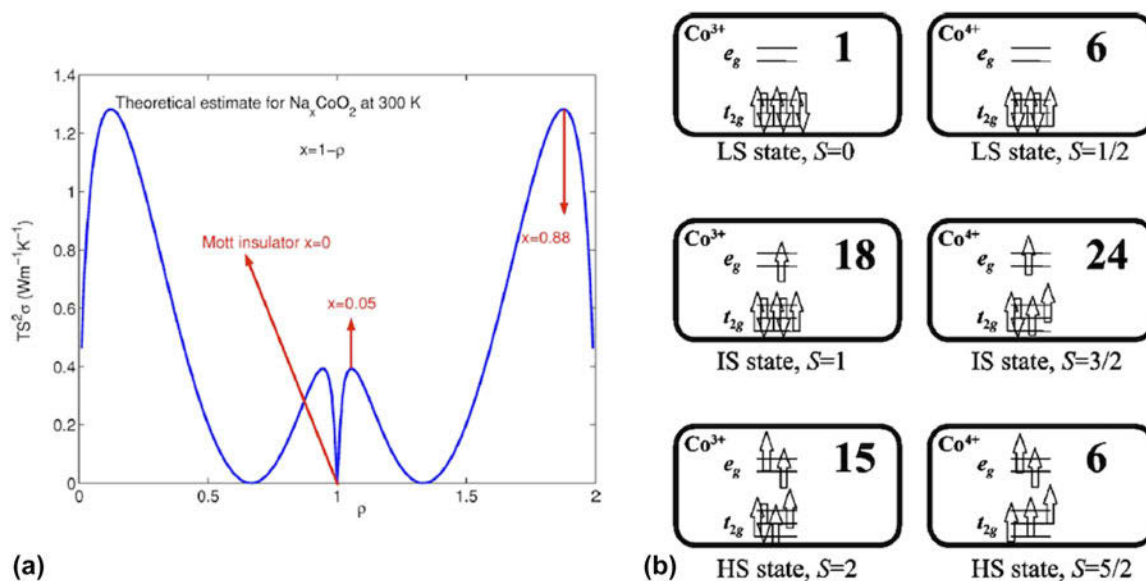


FIG. 3. (a) Doping dependence of thermoelectric power factor in  $\text{Na}_x\text{CoO}_2$ . The material is a band insulator for  $\rho = 0.2$ , and a Mott insulator for  $\rho = 1$ . The maximum obtained at  $\rho = 0.88$  agrees well with experimental results. Reprinted from Ref. 22 with the permission of AIP Publishing. (b) The calculated total degeneracy (spin + orbital) for cobaltates depending on their valence and spin configurations. The electronic configuration is shown for each case. Reprinted figure with permission from Ref. 24. Copyright (2000) by the American Physical Society.

spin transition that happens in perovskite cobaltates.<sup>77</sup> Further, the layered structure of these cobaltates leads to very low thermal conductivity,<sup>78</sup> as they follow the nano-structured block layered concept.<sup>79</sup> Thus, cobaltates have emerged as one of the important high efficiency p-type thermoelectric materials for high temperature applications.

### III. SYNTHESIS AND CHARACTERIZATION OF THERMOELECTRIC COMPLEX OXIDE THIN FILMS, HETEROSTRUCTURES, AND SUPERLATTICES

The synthesis of thin films and other low dimensional structures of complex oxides have been an important subject of investigation ever since the discovery of high- $T_c$  cuprates. Several thin film growth techniques such as molecular beam epitaxy,<sup>80–83</sup> pulsed laser deposition,<sup>84–86</sup> sputtering,<sup>87–93</sup> metal–organic chemical vapor deposition,<sup>94–98</sup> and chemical solution deposition<sup>99</sup> etc. have been used to synthesize high quality complex oxide thin films. As complex oxides have been of interest for a variety of applications, and physical phenomena, a range of synthesis techniques beyond what is discussed above could have been used. In this section, we will discuss some select synthesis and characterization investigations carried out on thin films of thermoelectric complex oxides.

#### A. Titanates

One of the widely studied complex oxides for thermoelectric applications is the titanate family. STO is a prototypical titanate, which shows large thermoelectric power factor over a wide range of temperatures.<sup>20,100–102</sup> Besides STO, other titanates such as  $\text{CaTiO}_3$ ,<sup>103,104</sup> and  $\text{BaTiO}_3$ <sup>105–107</sup> were also investigated for their thermoelectric properties. Apart from these studies on typical thin films, thermoelectric properties of other exotic low dimensional structures such as quantum wells, superlattices etc.<sup>108–113</sup> were also studied. After the discovery of large thermoelectric power factor in La doped STO,<sup>20</sup> several thin film oriented investigations were performed on doped STO using pulsed laser deposition method. As doped STO remains the best n-type oxide thermoelectric material, several in-depth investigations studied the effect of single dopant,<sup>100</sup> multiple dopants,<sup>101,114,115</sup> and their Ruddlesden–Popper phases<sup>116</sup> on the thermoelectric properties of STO based thin films. Interestingly, the very first exploration of thermoelectric properties of heavily Nb doped ternary phase diagram of  $\text{CaTiO}_3$ – $\text{SrTiO}_3$ – $\text{BaTiO}_3$  was carried out using pulsed laser deposition.<sup>117</sup> Other growth techniques such as sputtering,<sup>118</sup> and molecular beam epitaxy (MBE)<sup>119</sup> were successfully used to grow doped STO films. Especially, MBE grown films demonstrated large cryogenic thermopower due to

the phonon drag effect,<sup>120</sup> due to exquisite stoichiometry control. The thermal properties of undoped STO were studied using a variety of growth methods to verify the ability of each technique in producing high quality STO films.<sup>121,122</sup>

Thin film growth of titanates is a matured research area due to the persistent interest in titanates for ferroelectric applications, especially  $\text{Ba}_{1-x}\text{Sr}_x\text{TiO}_3$ . Several single crystalline substrates are available for the growth of titanates such as  $\text{CaTiO}_3$  ( $a_{\text{pc}} = 3.826 \text{ \AA}$ ) ( $a_{\text{pc}}$  refers to pseudocubic lattice parameter, which is an approximate cubic lattice parameter derived for orthorhombic unit cells),  $\text{SrTiO}_3$  ( $a = 3.905 \text{ \AA}$ ),  $\text{BaTiO}_3$  ( $a = 3.992 \text{ \AA}$ ), and their alloys. Fortunately,  $\text{SrTiO}_3$  is the widely used perovskite substrate, which is also a common substrate for several thermoelectric complex oxides. Besides STO, other single crystalline substrates such as  $\text{LaAlO}_3$  ( $a = 3.79 \text{ \AA}$ ),  $(\text{LaAlO}_3)_{0.3}(\text{Sr}_2\text{TaAlO}_6)_{0.7}$  (LSAT) ( $a = 3.868 \text{ \AA}$ ),  $\text{NdGaO}_3$  ( $a_{\text{pc}} = 3.863 \text{ \AA}$ ),  $\text{DyScO}_3$  ( $a_{\text{pc}} = 3.947 \text{ \AA}$ ),  $\text{GdScO}_3$  ( $a_{\text{pc}} = 3.961 \text{ \AA}$ ) etc. are widely used to cover the entire range of in-plane lattice parameters possible for the titanate thin film family. The epitaxial relationship between the titanates especially STO and various perovskite substrates can be often simplified as a cube-on-cube geometry.<sup>123</sup> Despite this advantage, the titanates are prone to be highly nonstoichiometric<sup>124</sup> with profound effect on this physical properties,<sup>121,125</sup> especially thermoelectric properties.<sup>101,126</sup> For example, in the case of STO, due to the presence of deep valence bands with respect to the vacuum level, only n-type doping is thermodynamically feasible.<sup>127</sup> Trivalent ions such as La, Pr on the A-site (Sr), pentavalent ions such as Nb on the B-site (Ti), oxygen vacancies, or a combination of these were used as common dopants to achieve n-type conduction in STO.<sup>100,101,114,118–120,126</sup> On the other hand, cationic vacancies can act as compensating defects.<sup>128–130</sup> Hence, understanding the effect of various point defects on the thermoelectric properties of such titanates has been an important issue. Often, it is difficult to elucidate how these defects are created, whether it is dictated by the growth process, thermodynamics, or if they arise from extrinsic causes such as doping/alloying, and other impurities. On top of these challenges, the lack of powerful analytical technique(s) to quantitatively characterize the point defect density and distribution hampers the understanding the interrelationship between point defects and physical properties. Hence, researchers often resort to a combination of techniques to elucidate the nature of point defects in these thermoelectric materials.

Some of the common structural characterization techniques used are x-ray diffraction (XRD), electron microscopy,<sup>124</sup> Rutherford backscattering,<sup>125</sup> ellipsometry,<sup>126,131</sup> etc. XRD remains the most powerful technique to characterize the bulk structural properties of thin films. This method has been widely used to study titanate thin

films; especially STO based thin film materials. Figure 4 shows the typical x-ray diffraction based characterization measurements performed on STO based thin films, which include typical Bragg scans ( $\theta$ - $2\theta$  scan), rocking curves,  $\phi$ -scan, and reciprocal space mapping. One can see that the effect of most doping schemes and/or nonstoichiometry is the expansion of the  $c$ -axis lattice parameter. The nonselectivity of this lattice expansion has been a subject of several investigations, and hence, limits to use of XRD to quantify the presence of different point defects in STO. Figure 5 summarizes other common characterization techniques such as high resolution scanning transmission electron microscopy, atomic force microscopy, Rutherford backscattering, and optical reflectivity to characterize STO based thin films. Often, a combination of both the structural, chemical probes along with physical property measurements have been more successful in providing some insights into the effect of defects on the thermal and thermoelectric properties.<sup>101,125,126,131</sup>

Other important factors affecting the thermoelectric properties include residual strain and defects created during strain relaxation, often via creation of dislocations.

## B. Cobaltates

Misfit layered cobaltates have a general structure consisting of CdI<sub>2</sub>-type CoO<sub>2</sub> layers sandwiched between rock-salt layers or in other cases, ions such as Li, Na etc. The prototypical member of this family is Na<sub>x</sub>CoO<sub>2</sub>, which showed large thermoelectric power<sup>21</sup> and created interest in the family of compounds. The epitaxy of cobaltates is a lot more challenging than titanates, due to their complicated crystal structure. Simpler compounds such as Na<sub>x</sub>CoO<sub>2</sub> have been more successful in achieving some form of in-plane epitaxial relationship with different single crystalline substrates. Synthesis of Na<sub>x</sub>CoO<sub>2</sub> thin films was carried out primarily using pulsed laser deposition, but other methods such as topotactic exchange,

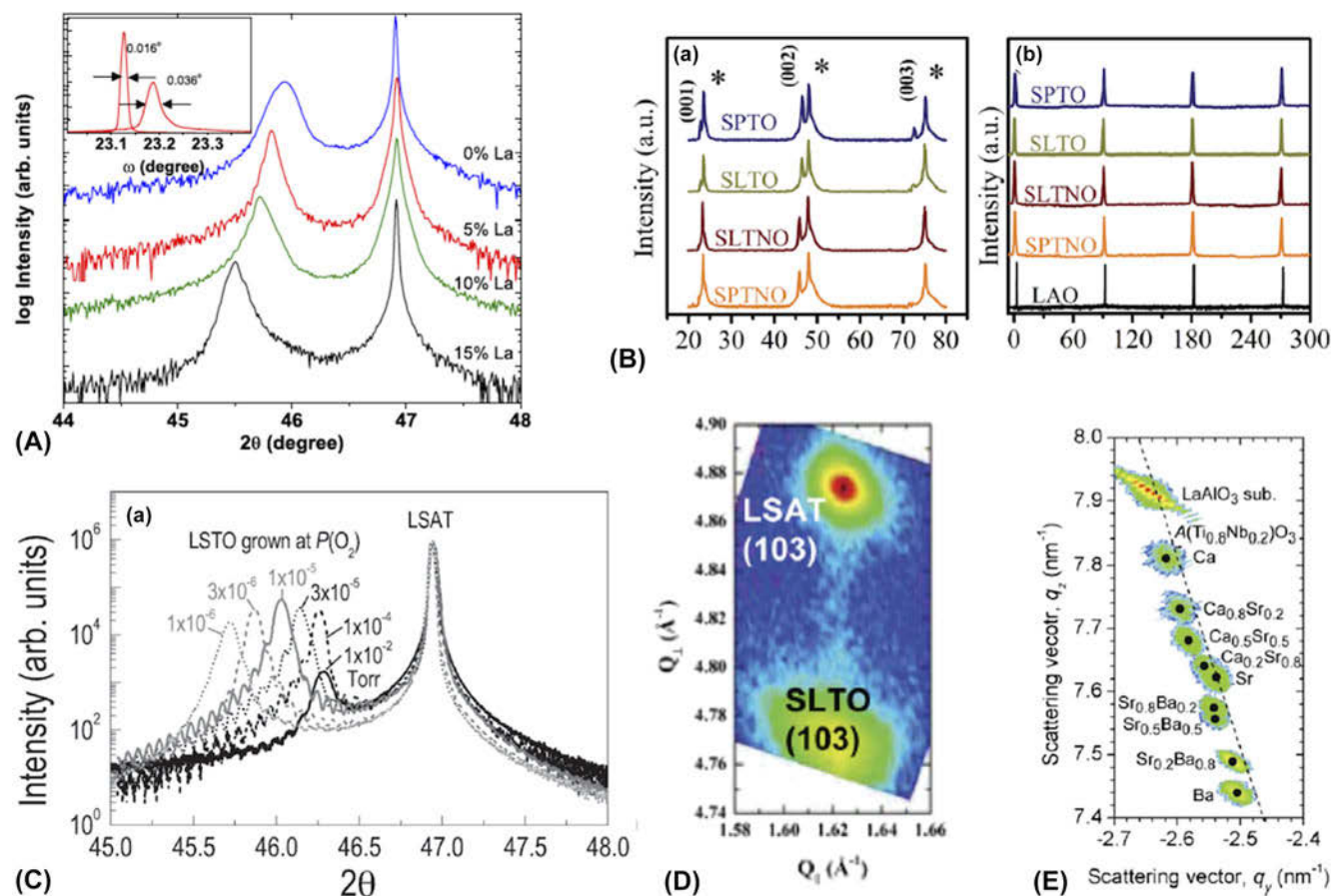


FIG. 4. (A) The evolution of 002 film peak for different La doping of “double doped” STO in a  $\theta$ - $2\theta$  scan; the inset shows the rocking curve for the film and substrate. Reprinted figure with permission from Ref. 101. Copyright (2010) by the American Physical Society. (B) The (left)  $\theta$ - $2\theta$  scan and (right)  $\phi$  scans for STO thin films on LAO with various dopants (Pr, La, La & Nb, and Pr & Nb). Reproduced from Ref. 114 with permission of The Royal Society of Chemistry. (C) The evolution of 002 film peak for different growth pressures for “double doped” STO with fixed La doping in a  $\theta$ - $2\theta$  scan. Reproduced from Ref. 126 with permission of Wiley Materials. (D) The reciprocal space map for 1 at% La doped STO film on LSAT substrate. Reprinted from Ref. 118 with the permission of AIP Publishing. (E) The reciprocal space map for various alloy compositions of Nb doped CaTiO<sub>3</sub>-SrTiO<sub>3</sub>-BaTiO<sub>3</sub> system. Reprinted from Ref. 117 with the permission of AIP Publishing.

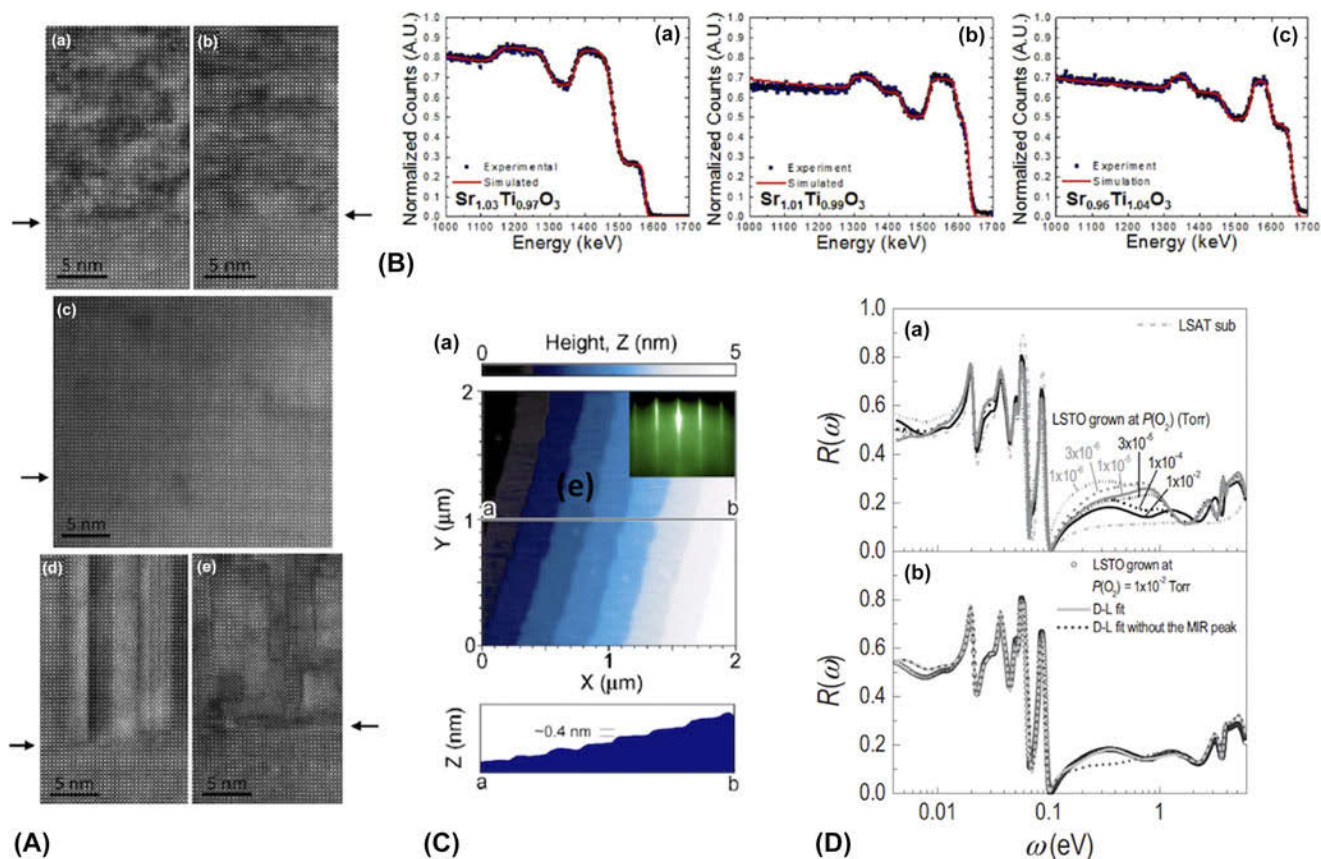


FIG. 5. (A) Scanning transmission electron micrograph of STO thin films with different stoichiometries [(a and b) strontium deficient, (c) stoichiometric, (d and e) strontium excess]. Reprinted from Ref. 124 with the permission of AIP Publishing. (B) Rutherford backscattering spectra for STO thin films with different levels of (non)stoichiometry. Reprinted with permission from Ref. 125. Copyright (2012) American Chemical Society. (C) Atomic force micrograph and (inset) typical reflection high energy electron diffraction pattern for the (Ca, Sr, Ba)  $\text{Ti}_{0.8}\text{Nb}_{0.2}\text{O}_3$  thin films. Reprinted from Ref. 117 with the permission of AIP Publishing. (D) The optical reflectivity curves for “double doped” STO with fixed La doping. Reproduced from Ref. 126 with permission of Wiley Materials.

chemical solution deposition.<sup>132–139</sup> Several attempts resulted in epitaxial growth of  $\text{Na}_x\text{CoO}_2$ , on *c*-plane sapphire,  $\text{SrTiO}_3$ ,  $\text{SrLaGaO}_4$  etc.<sup>132,133,137,140</sup> As sodium in these compounds is a reactive species, these films often suffered from poor stability. These stability issues were addressed using barrier or capping layers and the thermoelectric properties at room temperature were found to be largely stable and comparable to bulk single crystals.<sup>135</sup>

The thin film studies also focused on other notable layered cobaltates such as  $\text{Ca}_3\text{Co}_4\text{O}_9$ ,  $\text{Bi}_2\text{Sr}_2\text{Co}_2\text{O}_y$  etc. We will not focus our discussions on  $\text{Ca}_3\text{Co}_4\text{O}_9$ , as this material has received considerable attention in a recent review article,<sup>35</sup> but we will discuss the growth efforts on  $\text{Bi}_2\text{Sr}_2\text{Co}_2\text{O}_y$  and related compounds.<sup>141–150</sup> The common techniques used for the growth of cobaltates were pulsed laser deposition, chemical solution deposition, and RF sputtering. Figure 6 documents some of the x-ray ( $\theta$ – $2\theta$  scans and  $\phi$ -scans) and microscopic analyses performed on thin films of cobaltates. As one can see, perfect in-plane epitaxial relationship between the film and substrate was hard to achieve, due to the anisotropic

and complicated crystal structure of  $\text{Bi}_2\text{Sr}_2\text{Co}_2\text{O}_y$  unlike in  $\text{Na}_x\text{CoO}_2$ , where epitaxial growth was achieved. Also, film–substrate interface of  $\text{Bi}_2\text{Sr}_2\text{Co}_2\text{O}_y$  contained an amorphous layer, even though this didn’t affect the out-of-plane texturing and crystallinity of the films far from the interface.

### C. Other materials

Apart from titanates and cobaltates, the thin film studies on other materials have been rather limited. Even though thermopower is widely used as an important transport quantity, many transport studies were not primarily focused on thermoelectric properties. Hence, such studies are not reviewed in this article. Although doped  $\text{CaMnO}_3$ <sup>66–68</sup> is considered one of the important thermoelectric materials, there are few reports of thin film synthesis.<sup>151,152</sup> Interestingly, the idea of electron filtering to improve thermoelectric properties of superlattices was studied in the model system  $\text{La}_{0.67}\text{Sr}_{0.33}\text{MnO}_3/\text{LaMnO}_3$ .<sup>153,154</sup> Other materials studied include p-type conducting  $\text{CaAlO}_2$ ,<sup>155</sup>  $\text{LaCo}_{1-x}\text{Ni}_x\text{O}_3$ .<sup>156</sup>



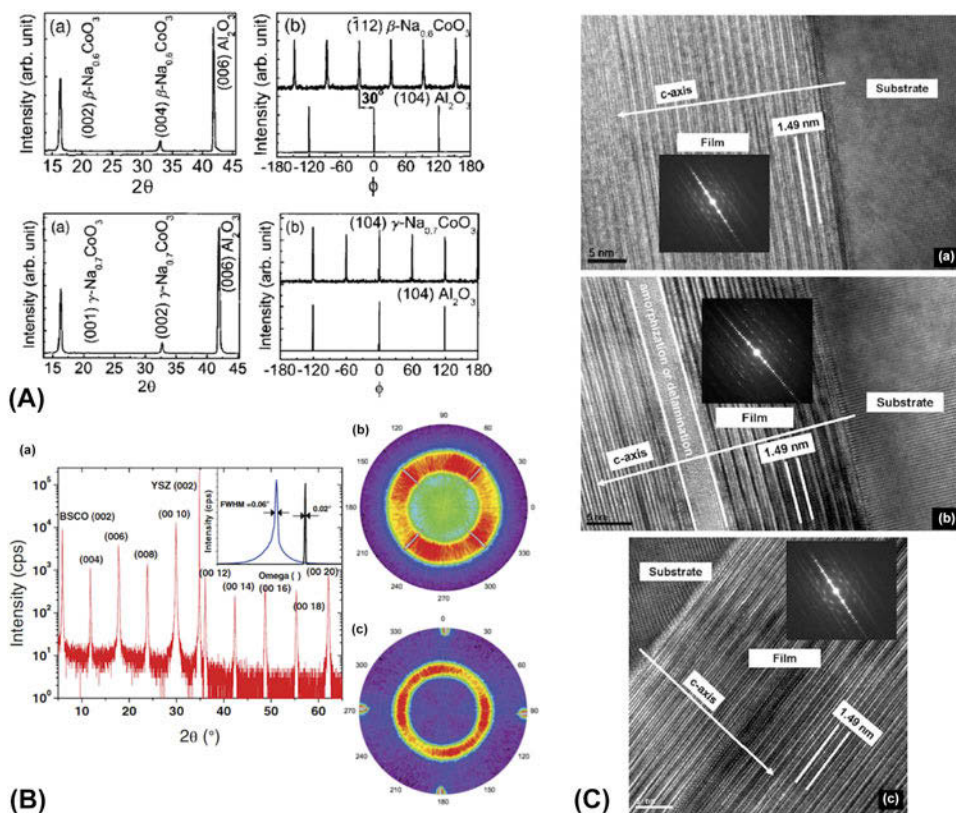


FIG. 6. (A) (Top panel) XRD pattern and  $\phi$ -scan for  $\beta$ - $\text{Na}_x\text{CoO}_2$  thin films. (Bottom panel) XRD pattern and  $\phi$ -scan for  $\gamma$ - $\text{Na}_x\text{CoO}_2$  thin films. Reprinted from Ref. 137 with the permission of AIP Publishing. (B) XRD pattern, pole figure scan, and rocking curve (inset) for  $\text{Bi}_2\text{Sr}_2\text{Co}_2\text{O}_y$  films on YSZ substrate. Reprinted figure with permission from Ref. 143. Copyright (2012) by the American Physical Society. (C) TEM images of  $\text{Bi}_2\text{Sr}_2\text{Co}_2\text{O}_y$  films grown on (a) STO (001), (b) STO (110), and (c) STO (111). Reprinted from Ref. 150, with permission from Elsevier.

#### IV. THERMOELECTRIC AND THERMAL TRANSPORT STUDIES

Thin film synthesis of oxide materials is a matured area of research, but the thermoelectric measurements on these thin films present unique challenges. Recent developments<sup>157–163</sup> in the thermoelectric metrology for thin films have played a critical role in enabling the studies detailed below.

##### A. Thermoelectric properties

The thermoelectric properties of thin film materials, especially that of titanates and cobaltates have been reported extensively. As discussed earlier, these investigations were concentrated on these materials exclusively, with few reports on other promising thermoelectric materials. Hence, this section will summarize thermoelectric transport measurement efforts on titanates and cobaltates.

As discussed earlier, doped  $\text{SrTiO}_3$  is one of the best n-type conducting oxide thermoelectric materials. Large effective mass in STO leads to high thermopower even in very large carrier densities ( $>10^{21} \text{ cm}^{-3}$ ), and hence, a large power factor.<sup>164</sup> We will discuss some

select investigations on doped STO, where extensive temperature dependent thermoelectric properties were reported. Ohta et al. performed one of the first investigations on the thermoelectric properties of Nb doped STO films.<sup>100</sup> Due to the solubility limitation of Nb on the B-site of STO, they used the thin film approach to stabilize a large Nb concentration of up to  $\sim 40\%$ . Although the study reported electrical conductivity, thermopower, Hall mobility, and carrier concentration, they estimated the thermal conductivity to be  $\sim 3 \text{ W/(m K)}$ . Thermal conductivity measurements in thin films of oxide materials are rather challenging, and we will discuss this aspect in more detail in Sec. IV. B. The highest  $ZT$  of 0.37 was achieved at 1000 K for the 20% Nb doped STO ( $\text{SrTi}_{0.8}\text{Nb}_{0.2}\text{O}_3$ ) and remains one of the highest  $ZT$  achieved in thin film form of STO. Ravichandran et al. reported the first comprehensive study of thermoelectric properties of thin films of doped STO, including thermal conductivity measurements. They used two dopants to explore the effect of both La on the A site, and the oxygen vacancies on thermoelectric properties, as typical single dopants were insufficient to achieve further enhancement of  $ZT$ . Oxygen vacancies

were incorporated in the La doped STO films by growing the films in varying amount of oxygen partial pressure. These were called as “double doped STO” and idea of using two dopants was to explore the possibility of band engineering in STO, beyond just the tuning of carrier density.<sup>165</sup> As the growth at low pressures can lead to other cationic vacancies such as Sr vacancies,<sup>126,128</sup> it is unclear whether the intended oxygen vacancies were the only type of defects achieved using this procedure. As Sr vacancies act as acceptors, they can act as competing defects in these films. This approach failed to produce any significant enhancement in the power factor, but significant reduction in thermal conductivity, especially at room temperature was observed. The room temperature  $ZT$  increased to 0.18 for 5% La doped STO ( $\text{La}_{0.05}\text{Sr}_{0.95}\text{TiO}_{3-\delta}$ ), compared to the earlier reported value of 0.1 in single crystals.<sup>20</sup> The highest  $ZT$  reported was 0.28 at 873 K. One of the important features of this study was the direct thermal conductivity measurements on the films using the TDTR method, to accurately deduce  $ZT$  for the films.<sup>157</sup> The summary of the reported thermoelectric properties (electrical and thermal conductivity, thermopower, power factor and  $ZT$ ) in this study is shown in Fig. 7. Similar study on the effect of La/Nb dopants along with oxygen vacancies was performed by Sarath Kumar et al., who used  $\text{O}_2/\text{Ar}$  mixture to control the oxygen vacancy content in the films.<sup>115</sup>

They estimated the highest  $ZT$  of 0.29 at 1000 K, as they did not report thermal conductivity values at 1000 K. Abutaha et al. extended this double doping idea through a mechanism of doping on both the A- and B-sites of STO (La/Pr on A-site and Nb on the B-site), demonstrating enhancement in thermoelectric properties for double doped samples as compared to samples with single dopant. Interestingly, the temperature dependence of power factor in this study showed a peak at  $\sim 600\text{--}700$  K, instead of the decreasing trend observed by Ravichandran et al.<sup>101</sup> All the thermoelectric properties except thermal conductivity were reported over a wide temperature range of 300–1000 K. The highest  $ZT$  reported in this study was 0.016 at room temperature, as the power factor of these films was an order magnitude lower than the highest power factor values achieved in STO. Lee et al. reported the effect of Nb doping on the thermoelectric properties of the Ruddlesden–Popper (RP) phase of STO,  $\text{Sr}_2\text{TiO}_4$ . Despite the possibility of lower thermal conductivity in RP phases, their power factor was lower than equivalently doped STO films. All the investigations were performed using pulsed laser deposition as the growth technique. All these studies used  $\text{LaAlO}_3$  (LAO) substrate (lattice mismatch of  $\sim 3\%$  with STO) except Ravichandran et al., who used LSAT substrates with a lower lattice mismatch with STO ( $<1\%$ ). Jalan et al. reported the first study on thermoelectric properties of

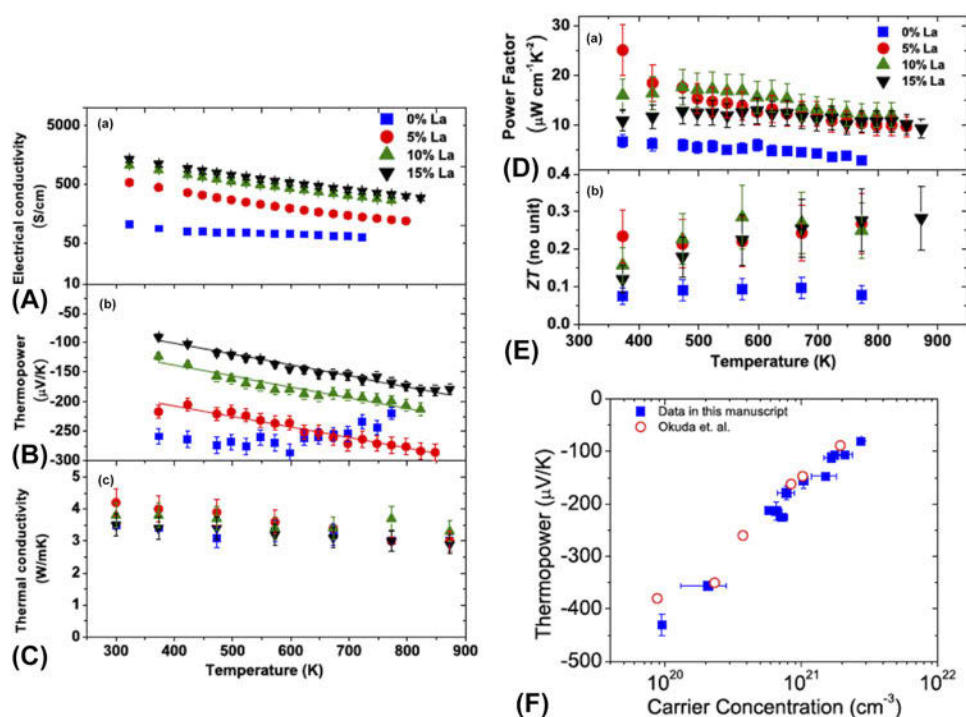


FIG. 7. Thermoelectric properties of “double doped” STO films. (A) Electrical resistivity, (B) thermopower, (C) thermal conductivity, and derived (D) power factor, and (E)  $ZT$  for “double doped” STO films over a temperature range of 300–900 K. (F) The evolution of thermopower with carrier density at room temperature and its comparison with the reported values in the literature. Reprinted figure with permission from Ref. 101. Copyright (2010) by the American Physical Society.

MBE grown doped STO films.<sup>119</sup> Although no thermal conductivity values were reported, this study achieved the highest power factor of  $39 \mu\text{W}/(\text{m K}^2)$  achieved in any form of doped STO at room temperature. Cain et al. was able to use the similar growth method to achieve very large cryogenic power factor of  $470 \mu\text{W}/(\text{m K}^2)$ , especially due to the realization of phonon drag effect.<sup>120</sup>

The second materials family is the layered cobaltate family, which is the best p-type conducting oxide thermoelectric materials system. There are few reviews, which cover some aspects of this materials system, such as  $\text{Ca}_3\text{Co}_4\text{O}_9$  thin films,<sup>31,35</sup> and cobaltate thin films prepared by reactive solid-phase epitaxy with topotactic ion-exchange methods.<sup>166</sup> Hence, this section will focus on studies, which are not covered by these reviews. Although much of the interest in this materials system stemmed from the large thermoelectric power factor in  $\text{Na}_x\text{CoO}_2$ ,<sup>21,73</sup> most thin film synthesis efforts were affected by the poor stability of  $\text{Na}_x\text{CoO}_2$ .<sup>135</sup> Hence, only few studies addressed the thermoelectric properties in detail, and often below room temperature.<sup>134,136</sup>

Venimadhav et al.<sup>134</sup> prepared  $\text{Na}_x\text{CoO}_2$  thin films using two different techniques: one using a two-step topotaxial conversion of  $\text{Co}_3\text{O}_4$  films into  $\text{Na}_x\text{CoO}_2$ , and another of direct synthesis. Both methods used pulsed laser deposition for the synthesis. The reported thermopower and electrical conductivity were lower than the values reported for single crystals, presumably due to difficulties associated with controlling the sodium content in the films, which has profound influence on the thermoelectric properties.<sup>73</sup> Brinks et al.<sup>136</sup> studied the effect of substrate symmetry and lattice constants on the thermoelectric properties of  $\text{Na}_x\text{CoO}_2$  films, and found that even cubic substrates were suitable for epitaxial growth of  $\text{Na}_x\text{CoO}_2$  films. The highest  $ZT$  obtained was  $\sim 0.17$  at room temperature for films grown on LSAT substrates. In conclusion, further studies are required to understand mechanisms to stabilize films with high Na content, and to realize higher figure of merit in the thin films of  $\text{Na}_x\text{CoO}_2$  system. Due to inherent stability issues of  $\text{Na}_x\text{CoO}_2$ , which becomes more pronounced in the thin film form, several research groups focused on other stable cobaltate systems such as  $\text{Ca}_3\text{Co}_4\text{O}_9$ ,  $\text{Bi}_2\text{Sr}_2\text{Co}_2\text{O}_y$  etc.

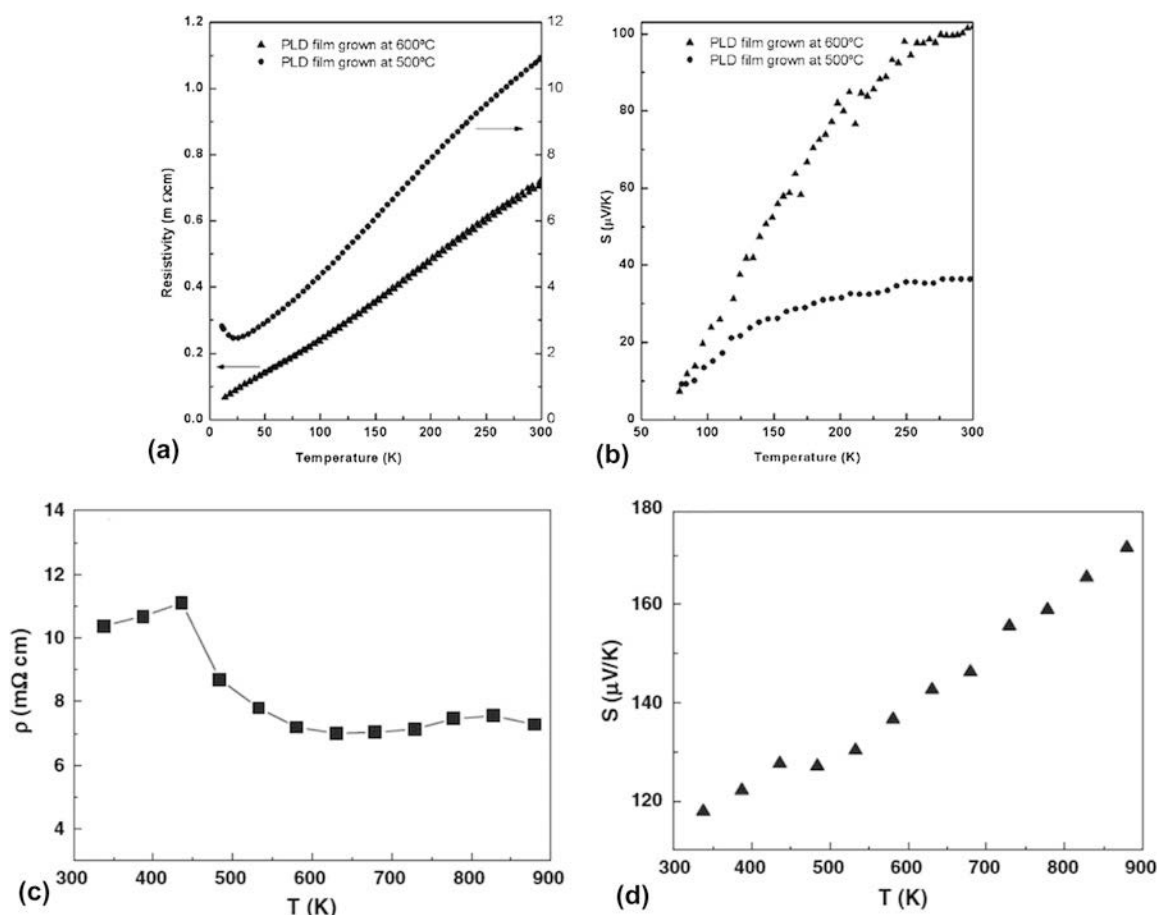


FIG. 8. Low temperature (a) electrical resistivity and (b) thermopower of PLD grown  $\text{Na}_x\text{CoO}_2$  thin films. Reproduced with permission from Ref. 134. High temperature (c) electrical resistivity and (d) thermopower of  $\text{Bi}_2\text{Sr}_2\text{Co}_2\text{O}_y$  thin films. Reprinted from Ref. 142, with permission from Elsevier.

An interesting aspect of the cobaltate materials is the anisotropic transport properties. To study this anisotropy, Sakai et al. prepared  $\text{Sr}_3\text{Co}_4\text{O}_9$  films on  $c$ -plane,  $a$ -plane, and  $m$ -plane sapphire substrates and studied their temperature dependent thermoelectric properties (below room temperature).<sup>146</sup> Wang et al. carried out one of the first investigations on the thin films of  $\text{Bi}_2\text{Sr}_2\text{Co}_2\text{O}_y$ . Interestingly, they were able to grow textured films even on amorphous fused silica substrate, besides single crystalline LAO substrate, but the transport properties were superior on LAO substrates, and were comparable to the single crystal properties.<sup>27</sup> Wang et al. prepared

nanocrystalline thin films of  $\text{Bi}_2\text{Sr}_2\text{Co}_2\text{O}_y$  on LAO substrate through chemical solution deposition, and studied its thermoelectric properties above room temperature.<sup>142</sup> These films showed higher power factor compared to the polycrystalline materials, and likely had very low thermal conductivity due to the nanocrystalline nature. Shu-Fang et al. studied the effect of oxygen annealing on the thermoelectric properties of chemical solution deposited thin films of  $\text{Bi}_2\text{Sr}_2\text{Co}_2\text{O}_y$  on LAO substrate.<sup>149</sup> They found modest increase in the thermoelectric properties upon annealing at high temperature. The summary of thermoelectric properties (electrical conductivity and

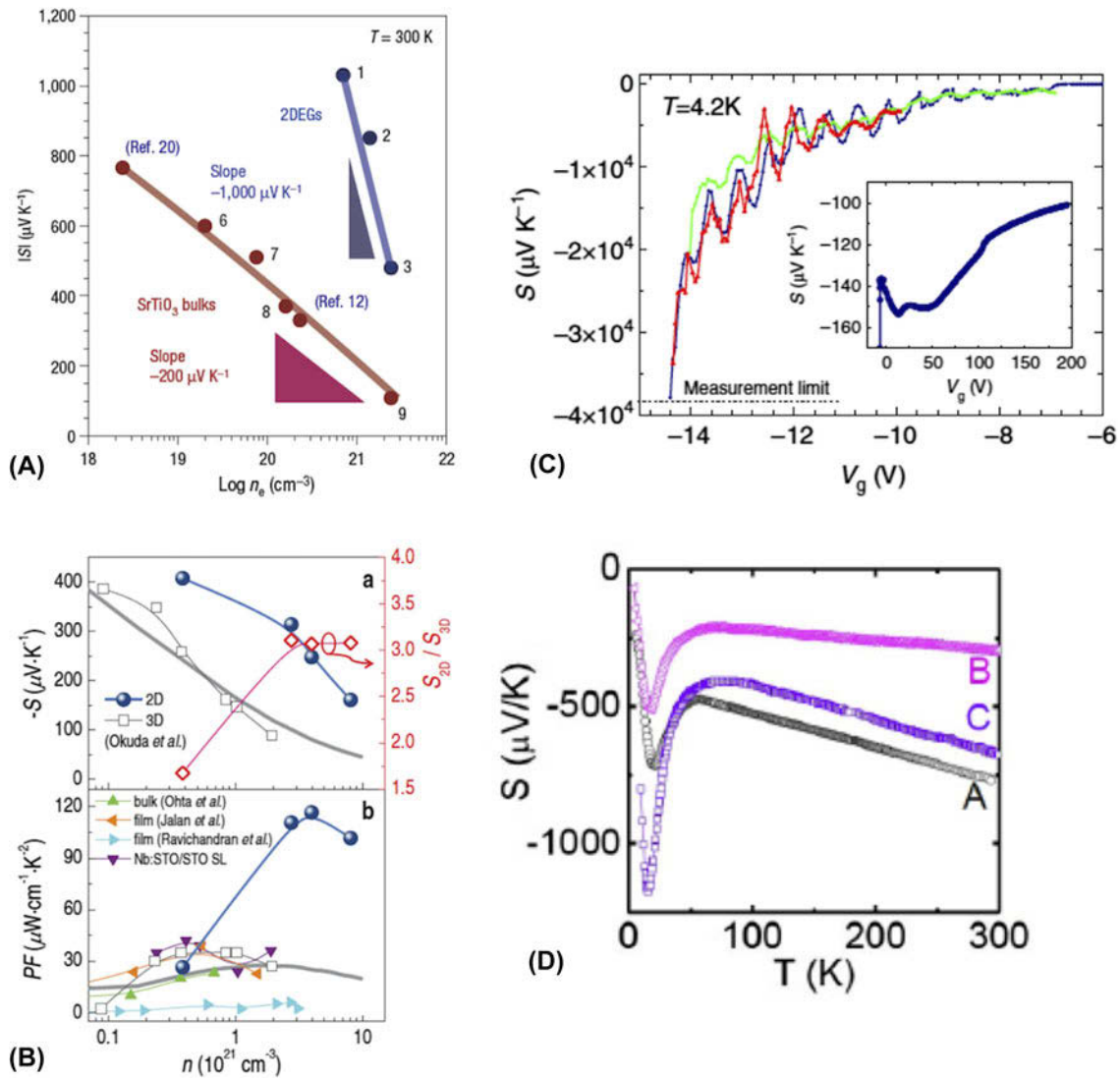


FIG. 9. (A) Comparison of thermopower in bulk and quantum confined superlattices of Nb:SrTiO<sub>3</sub>/SrTiO<sub>3</sub>. Reprinted with permission from Macmillan Publishers Ltd: Nature Materials (Ref. 108), copyright (2007). (B) Thermoelectric properties of bulk and low dimensional (2D) thermoelectric oxides. (a) Thermopower and (b) power factor as a function of carrier density for bulk samples (empty squares) and fractional superlattices (filled circles). Reproduced from Ref. 171 with permission of Wiley Materials. (C) Seebeck coefficient as a function of gate voltage measured in a LAO/STO heterostructure at 4.2 K. The plot clearly shows giant oscillations in the Seebeck coefficient upon tuning of carrier density. Reproduced from Ref. 175 with permission from Nature Publication Group. (D) Seebeck coefficient measured as a function of temperature for LAO/STO samples with different carrier density. The large “phonon drag” peak is evident at low temperatures. Reprinted figure with permission from Ref. 176. Copyright (2016) by the American Physical Society.

thermopower) reported for  $\text{Na}_x\text{CoO}_2$ , and  $\text{Bi}_2\text{Sr}_2\text{Co}_2\text{O}_y$  are shown in Fig. 8.<sup>134,141,142</sup>

### B. Thermal properties

Thermal property measurements for oxide thin films, especially epitaxial films, are challenging due to limited availability of reliable measurement techniques. Recent advances in thermal metrology<sup>157–160</sup> have enabled some of the investigations, especially  $\text{SrTiO}_3$  based thin films. Hence, in this section, we will focus on the thermal measurements performed on thin film STO based materials. Although the development of  $3\omega$  technique enabled wide availability of thermal metrology for thin film materials,<sup>158</sup> it was not suitable for most epitaxial oxide thin films, due to low thermal conductivity mismatch between the film and the substrate materials. In certain situations, STO thin films grown on STO templated Si substrates were suitable for thermal conductivity measurements.<sup>167</sup> Time domain thermoreflectance was more appropriate and easier to implement for oxide thin films,

due to the smaller thermal penetration depth over which the metrology is carried out.<sup>157</sup> Several research groups used TDTR technique to measure the thermal conductivity of epitaxial and/or ultrathin oxide thin films. Oh et al. reported one of the most comprehensive survey of low temperature thermal conductivity (room temperature and below) for epitaxial  $\text{SrTiO}_3$  thin films grown by PLD and MBE techniques.<sup>121</sup> This study showed that the highest quality STO thin films grown by both growth techniques were comparable within the limits of thermal conductivity as a quality metric. Further, they also showed that the growth-induced defects affected the thermal conductivity of STO significantly at room temperature, especially while using PLD to grow STO films. Detailed thermal conductivity measurements on “double doped” STO enabled direct determination of  $ZT$  up to  $\sim 900$  K.<sup>101</sup> The effect of defects on the thermal properties of epitaxial films was studied in detail for PLD<sup>125</sup> and MBE<sup>168</sup> grown STO films. Foley et al. studied the thermal properties of nano-grained STO films prepared by chemical solution deposition, and showed strong grain size dependent

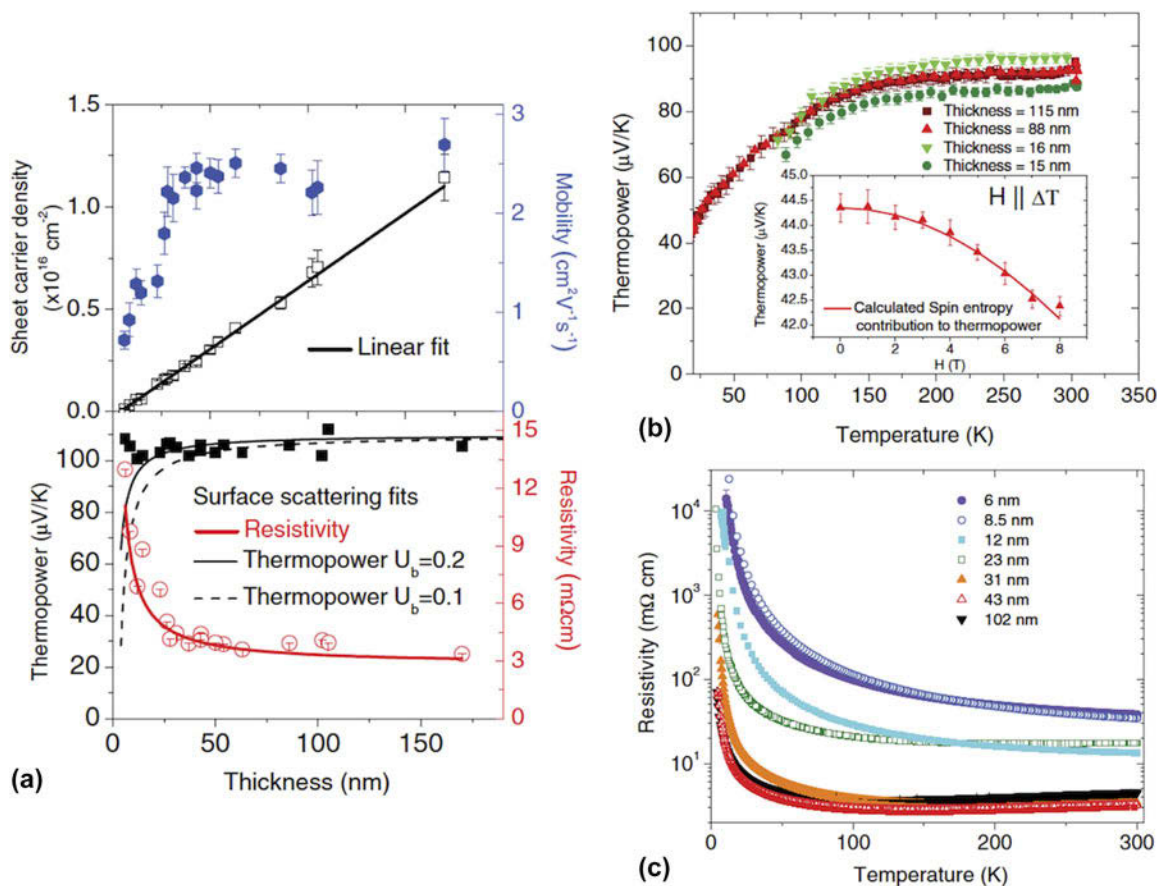


FIG. 10. (a) Evolution of (top) sheet carrier density and Hall mobility, and (bottom) thermopower and resistivity for  $\text{Bi}_2\text{Sr}_2\text{Co}_2\text{O}_y$  thin films as a function of film thickness. The mobility has a linear fit, and the resistivity and thermopower values are fit using a surface scattering model. (b) Low temperature thermopower for  $\text{Bi}_2\text{Sr}_2\text{Co}_2\text{O}_y$  thin films with different thicknesses. (Inset) Magnetic field dependent thermopower and the fit for spin entropy model. (c) The temperature dependent resistivity for  $\text{Bi}_2\text{Sr}_2\text{Co}_2\text{O}_y$  thin films with different thicknesses. Reprinted figure with permission from Ref. 143. Copyright (2012) by the American Physical Society.

thermal properties.<sup>169</sup> These studies established TDTR as the preferred thermal metrology technique for oxide films with thicknesses of few hundred nanometers or less.

### C. Size effects and low dimensional materials

The size effects have important effect on the thermal and thermoelectric properties. Hicks and Dresselhaus predicted that large thermoelectric power factor can be achieved in low dimensional materials.<sup>10,11</sup> We will review some of the interesting studies on low dimensional systems such as superlattices, and ultrathin films and how the thermoelectric properties are influenced by the low dimensionality.

Two dimensional electron gases (2DEG) are dimensionally confined systems, which can show enhanced thermoelectric properties as predicted by Hicks and Dresselhaus. Ohta et al. reported large thermopower

values in 2DEGs of dimensionally confined Nb doped STO layers in an Nb:STO/STO superlattice system.<sup>108</sup> This study showed a plausible mechanism for achieving large figure of merit in superlattice systems. Further studies expanded the phase space over which thermoelectric properties of the Nb:STO/STO superlattice system was studied.<sup>109,170</sup> Recently, Choi et al. expanded this line of study by realizing large power factor in fractionally  $\delta$ -doped superlattices of La:STO/STO.<sup>171</sup> Although these studies highlight enhanced thermoelectric properties in dimensionally confined electron gases, further studies are required to identify how can we use such superlattices containing 2DEGs for crafting devices with large thermoelectric efficiency. Another interesting system, which is related to this idea, is the LAO/STO heterostructure.<sup>172</sup> Over the years, this system has been intensely studied due to its fascinating physical properties, but has remained a controversial area of research. Several studies documented

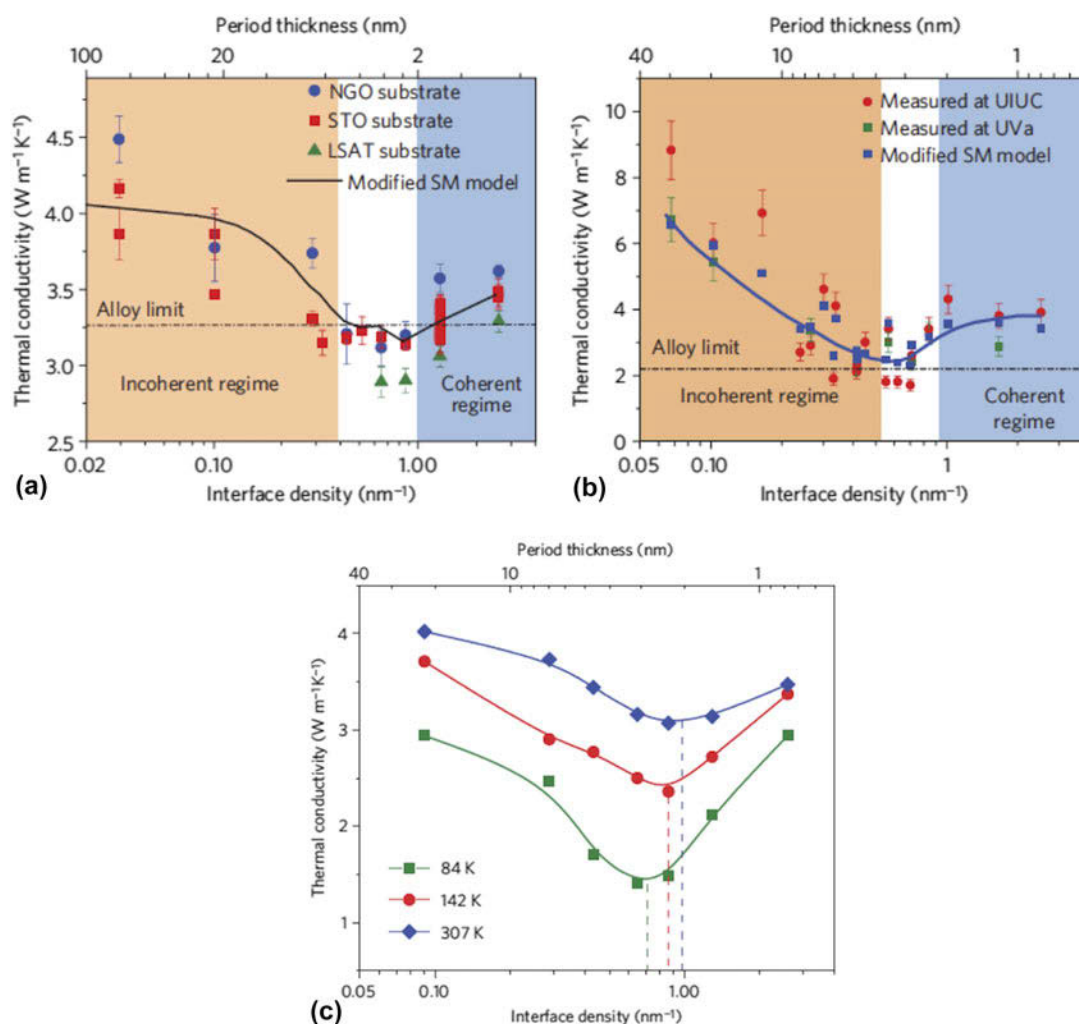


FIG. 11. Measured thermal conductivity values for (a) SrTiO<sub>3</sub>/CaTiO<sub>3</sub> and (b) SrTiO<sub>3</sub>/BaTiO<sub>3</sub> superlattices as a function of interface density at room temperature. (c) Temperature dependence of measured thermal conductivity values for SrTiO<sub>3</sub>/CaTiO<sub>3</sub> superlattices as a function of interface density. Reprinted with permission from Nature Publication Group (Nature Materials) (Ref. 111), copyright (2014).

the Seebeck effect in LAO/STO interface<sup>173</sup> including anomalous thermoelectric behavior,<sup>174</sup> quantum oscillations in thermopower,<sup>175</sup> large phonon drag thermopower enhancement<sup>176</sup> etc. Related to LAO/STO, GdTiO<sub>3</sub>/SrTiO<sub>3</sub> heterostructures were also studied in detail and found to demonstrate large thermopower values ( $\sim 300$   $\mu\text{V}/\text{K}$ ) despite showing large 2D sheet carrier densities.<sup>177</sup> Fig. 9 shows various interesting thermoelectric phenomena observed in low dimensional STO. These studies underpin how dimensionally confined STO remains an interesting system for demonstrating interesting low dimensional thermoelectric behavior. Besides STO, cobaltates have been subject of investigations related to low dimensionality. Ravichandran et al. performed thickness dependent thermoelectric property investigations on Bi<sub>2</sub>Sr<sub>2</sub>Co<sub>2</sub>O<sub>y</sub> films and found that despite the resistivity increase due to surface scattering, thermopower remained unaffected. They attributed the strongly correlated nature of this material to the insensitivity of thermopower to surface scattering. Typically, in conventional materials, thermopower is sensitive to the variation in scattering mechanisms, unless the scattering process is energy independent. In the case of strongly correlated materials, whose thermoelectric behavior is explained by the Heikes formula,<sup>65</sup> thermopower is insensitive to scattering mechanisms. This phenomenon was verified by Brinks et al. by studying the thickness dependent thermoelectric properties of Na<sub>x</sub>CoO<sub>2</sub>.<sup>178</sup> Fig. 10 shows the demonstration related to insensitivity of thermopower to scattering mechanisms in correlated cobaltate thin films.

There are few reports documenting the effect of low dimensionality on thermal properties of oxide materials. Ravichandran et al. studied the effect of interfaces in oxide superlattices on the cross-plane phonon thermal conductivity across the interfaces by varying the interface density, while keeping the volume fraction of the two constituent materials constant.<sup>111</sup> This study experimentally demonstrated the theoretical prediction of a crossover in phonon scattering mechanism from incoherent to coherent processes.<sup>179</sup> Simkin and Mahan theorized that the experimental signature of this phenomenon is a minimum in thermal conductivity as one decreases the period thickness of superlattice to a length scale comparable or below the phonon mean free path. Ravichandran et al. showed the first experimental demonstration of these signatures, as shown in Fig. 11. This study provides an exciting opportunity to employ coherent phonon processes as a means to tailor thermal properties of superlattices, which is interesting for thermoelectrics, thermal management and phonon optics.

## V. CONCLUSION AND OUTLOOK

The development of thin film synthesis methods and transport metrology techniques over the last few decades

have played an important role in the evolution of thin film thermoelectrics as an active research area. Although such developments have been cursorily mentioned in the review, they remain the major foundation for several research areas including thermoelectrics. This is especially true for complex oxides, which are emergent thermoelectric materials compared to known thermoelectric chalcogenides such as Bi<sub>2</sub>Te<sub>3</sub>, PbTe etc. The emergence of oxides underpins the importance of not just new materials discovery, but also realizing and understanding the physical properties of known materials under a variety of conditions (doping, alloying, nanostructuring etc.) to discover new functionalities in known materials. For example, the large thermoelectric power factor in SrTiO<sub>3</sub> (Ref. 20) was experimentally realized about 40 years after several in depth transport studies were performed on SrTiO<sub>3</sub>,<sup>51-53</sup> including superconductivity.<sup>180</sup> Thus, we have every reason to believe that the research on new thermoelectric materials and phenomena will continue to provide unexpected results. The inherent complexity of the structure and chemistry of oxides provide an exciting playground for materials design, which is full of challenges and opportunities at the same time. The improvements in computational materials science and sheer computing power available have been an important driver not only for new materials discovery, but also to unravel the subtle interplay in the structural, chemical, electronic, and magnetic degree of freedom at play in these materials. Even though this synergy was not discussed in this review, the convergence of computational approaches and cutting edge experimental approaches will play an increasing role in understanding this interplay and use that knowledge to help realize the full potential of thin film oxide thermoelectrics.

Interesting physical phenomena related to quantum mechanical processes or wave behavior is always important to push the frontier of our understanding and enable new technologies. Thermoelectric research, especially thermal transport can gain tremendously by focusing on these new emerging research directions. The development and proliferation of nanoscale heat transport techniques and methodology have been one of the key reasons for successful application of nanoscale materials toward thermoelectrics and thermal transport research. One can envision that such novel approaches will continue to enrich our understanding of how electrons and phonons behave in these materials and will have lasting impact on research areas beyond what is discussed in this article.

Last but not least, the domain of application for thin film thermoelectrics is increasing and has grown beyond waste heat recovery. Hence, there is an increasing need to develop materials and structures with high figure of merit over a wide range of temperature, stability, and other

characteristics. Particularly, one can envision the application of using oxide thermoelectrics in harsh environmental conditions as sensors, active energy harvesting device etc. due to their chemical stability. Even though there is a high propensity for thermoelectric researchers to focus on creating materials with high figure of merit, it is useful to identify creative means to employ known thermoelectric materials for applications beyond waste heat recovery. Currently, the need for fundamental understanding of material properties is as equally important as the ability to develop scalable, inexpensive manufacturing process to develop devices and products from these high performance materials. Besides such methods will impact areas beyond thermoelectrics such as electronic, and optical materials and devices.

## ACKNOWLEDGMENTS

This work was supported by U.S. Department of Energy, Office of Science, Basic Energy Sciences, Materials Sciences and Engineering Division and a startup grant from Viterbi School of Engineering, University of Southern California.

## REFERENCES

1. D.M. Rowe: *CRC Handbook of Thermoelectrics* (CRC Press, 1995).
2. G.J. Snyder and E.S. Toberer: Complex thermoelectric materials. *Nat. Mater.* **7**, 105 (2008).
3. C.M. Bhandari: Minimizing the thermal conductivity. In *CRC Handbook of Thermoelectrics*, D.M. Rowe, ed. (CRC Press: Boca Raton, 1995).
4. D. Rowe and C. Bhandari: Optimization of carrier concentration. In *CRC Handbook of Thermoelectrics*, D.M. Rowe, ed. (CRC Press, Boca Raton, 1995).
5. L.E. Bell: Cooling, heating, generating power, and recovering waste heat with thermoelectric systems. *Science* **321**, 1457 (2008).
6. G. Slack: New materials and performance limits for thermoelectric cooling. In *CRC Handbook of Thermoelectrics*, D.M. Rowe ed.; CRC Press: 1995.
7. G.S. Nolas, J.L. Cohn, G.A. Slack, and S.B. Schujman: Semiconducting Ge Clathrates: Promising candidates for thermoelectric applications. *Appl. Phys. Lett.* **73**, 178 (1998).
8. J.L. Cohn, G.S. Nolas, V. Fessatidis, T.H. Metcalf, and G.A. Slack: Glasslike heat conduction in high-mobility crystalline semiconductors. *Phys. Rev. Lett.* **82**, 779 (1999).
9. G.S. Nolas, J.L. Cohn, G.A. Slack, and S.B. Schujman: Skutterudites: A phonon-glass-electron crystal approach to advanced thermoelectric energy conversion applications. *Annu. Rev. Mater. Sci.* **29**, 89 (1999).
10. L. Hicks and M. Dresselhaus: Effect of quantum-well structures on the thermoelectric figure of merit. *Phys. Rev. B: Condens. Matter Mater. Phys.* **47**, 12727 (1993).
11. L. Hicks and M. Dresselhaus: Thermoelectric figure of merit of a one-dimensional conductor. *Phys. Rev. B: Condens. Matter Mater. Phys.* **47**, 16631 (1993).
12. T. Harman, D. Spears, and M. Manfra: High thermoelectric figures of merit in PbTe quantum wells. *J. Electron. Mater.* **25**, 1121 (1996).
13. R. Venkatasubramanian, E. Siivola, T. Colpitts, and B. O'quinn: Thin-film thermoelectric devices with high room-temperature figures of merit. *Nature* **413**, 597 (2001).
14. K.F. Hsu, S. Loo, F. Guo, W. Chen, J.S. Dyck, C. Uher, T. Hogan, E.K. Polychroniadis, and M.G. Kanatzidis: Cubic  $\text{AgPb}_m\text{SbTe}_{2+m}$ : Bulk thermoelectric materials with high figure of merit. *Science* **303**, 818 (2004).
15. K. Biswas, J. He, I.D. Blum, C-I. Wu, T.P. Hogan, D.N. Seidman, V.P. Dravid, and M.G. Kanatzidis: High-performance bulk thermoelectrics with all-scale hierarchical architectures. *Nature* **489**, 414 (2012).
16. C. Vineis, A. Shakouri, and A. Majumdar: Nanostructured thermoelectrics: Big efficiency gains from small features. *Adv. Mater.* **22**, 3970 (2010).
17. M.W. Gaultois, T.D. Sparks, C.K.H. Borg, R. Seshadri, W.D. Bonificio, and D.R. Clarke: Data-driven review of thermoelectric Materials: Performance and resource considerations. *Chem. Mater.* **25**, 2911 (2013).
18. S.K. Yee, S. LeBlanc, K.E. Goodson, and C. Dames: \$ per W metrics for thermoelectric power generation: Beyond ZT. *Energy Environ. Sci.* **6**, 2561 (2013).
19. S. LeBlanc, S.K. Yee, M.L. Scullin, C. Dames, and K.E. Goodson: Material and manufacturing cost considerations for thermoelectrics. *Renewable Sustainable Energy Rev.* **32**, 313 (2014).
20. T. Okuda, K. Nakanishi, S. Miyasaka, and Y. Tokura: Large thermoelectric Response of metallic perovskites:  $\text{Sr}_{1-x}\text{La}_x\text{TiO}_3$  ( $0 < x < 0.1$ ). *Phys. Rev. B: Condens. Matter Mater. Phys.* **63**, 113104 (2001).
21. I. Terasaki, Y. Sasago, and K. Uchinokura: Large thermoelectric power in  $\text{NaCo}_2\text{O}_4$  single crystals. *Phys. Rev. B: Condens. Matter Mater. Phys.* **56**, R12685 (1997).
22. S. Mukerjee and J.E. Moore: Doping dependence of thermopower and thermoelectricity in strongly correlated materials. *Appl. Phys. Lett.* **90**, 112107 (2007).
23. W. Koshibae and S. Maekawa: Effects of spin and orbital degeneracy on the thermopower of strongly correlated systems. *Phys. Rev. Lett.* **87**, 236603 (2001).
24. W. Koshibae, K. Tsutsui, and S. Maekawa: Thermopower in cobalt oxides. *Phys. Rev. B: Condens. Matter Mater. Phys.* **62**, 6869 (2000).
25. I. Chowdhury, R. Prasher, K. Lofgreen, G. Chrysler, S. Narasimhan, R. Mahajan, D. Koester, R. Alley, and R. Venkatasubramanian: On-chip cooling by superlattice-based thin-film thermoelectrics. *Nat. Nanotechnol.* **4**, 235 (2009).
26. D. Miorandi, S. Sicari, F. De Pellegrini, and I. Chlamtac: Internet of things: Vision, applications and research challenges. *Ad Hoc Netw.* **10**, 1497 (2012).
27. K. Koumoto, I. Terasaki, and R. Funahashi: Complex oxide materials for potential thermoelectric applications. *MRS Bull.* **31**, 206 (2006).
28. K. Koumoto, Y. Wang, R. Zhang, A. Kosuga, and R. Funahashi: Oxide thermoelectric materials: A nanostructuring approach. *Annu. Rev. Mater. Res.* **40**, 363 (2010).
29. K. Koumoto: Oxide Thermoelectrics. In *Thermoelectrics Handbook*, D.M. Rowe, ed. (CRC Press, Boca Raton, 2005); pp. 1–15.
30. K. Koumoto, R. Funahashi, E. Guilmeau, Y. Miyazaki, A. Weidenkaff, Y. Wang, and C. Wan: Thermoelectric ceramics for energy harvesting. *Ann. Phys.* **96**, 1 (2012).
31. H. Ohta, K. Sugiura, and K. Koumoto: Recent progress in oxide thermoelectric materials: p-type  $\text{Ca}_3\text{Co}_4\text{O}_9$  and n-type  $\text{SrTiO}_3^-$ . *Inorg. Chem.* **47**, 8429 (2008).
32. S. Walia, S. Balendhran, H. Nili, S. Zhuiykov, G. Rosengarten, Q.H. Wang, M. Bhaskaran, S. Sriram, M.S. Strano, and K. Kalantar-zadeh: Transition metal oxides—Thermoelectric properties. *Prog. Mater. Sci.* **58**, 1443 (2013).



33. J.W. Fergus: Oxide materials for high temperature thermoelectric energy conversion. *J. Eur. Ceram. Soc.* **32**, 525 (2012).
34. S. Lee, J.A. Bock, S. Trolier-Mckinstry, and C.A. Randall: Ferroelectric-thermoelectricity and Mott transition of ferroelectric oxides with high electronic conductivity. *J. Eur. Ceram. Soc.* **32**, 3971 (2012).
35. P. Mele: Nanostructured thin films of thermoelectric oxides. In *Oxide Thin Films, Multilayers, and Nanocomposites*, P. Mele, T. Endo, S. Arisawa, C. Li, and T. Tsuchiya, eds. (Springer International Publishing, Cham, 2015); pp. 123–155.
36. W. Liu, X. Yan, G. Chen, and Z. Ren: Recent advances in thermoelectric nanocomposites. *Nano Energy* **1**, 42 (2012).
37. H. Alam and S. Ramakrishna: A review on the enhancement of figure of merit from bulk to nano-thermoelectric materials. *Nano Energy* **2**, 190 (2013).
38. P. Pichanusakorn and P. Bandaru: Nanostructured thermoelectrics. *Mater. Sci. Eng., R* **67**, 19 (2010).
39. M.G. Kanatzidis: Nanostructured thermoelectrics: The new paradigm? *Chem. Mater.* **22**, 648 (2010).
40. Y. Lan, A.J. Minnich, G. Chen, and Z. Ren: Enhancement of thermoelectric figure-of-merit by a bulk nanostructuring approach. *Adv. Funct. Mater.* **20**, 357 (2010).
41. M.S. Dresselhaus, G. Chen, M.Y. Tang, R.G. Yang, H. Lee, D.Z. Wang, Z.F. Ren, J.P. Fleurial, and P. Gogna: New directions for low-dimensional thermoelectric materials. *Adv. Mater.* **19**, 1043 (2007).
42. J.P. Heremans, V. Jovovic, E.S. Toberer, A. Saramat, K. Kurosaki, A. Charoenphakdee, S. Yamanaka, and G.J. Snyder: Enhancement of thermoelectric efficiency in PbTe by distortion of the electronic density of states. *Science* **321**, 554 (2008).
43. Y. Pei, X. Shi, A. Lalonde, H. Wang, L. Chen, and G.J. Snyder: Convergence of electronic bands for high performance bulk thermoelectrics. *Nature* **473**, 66 (2011).
44. Y. Pei, H. Wang, and G.J. Snyder: Band engineering of thermoelectric materials. *Adv. Mater.* **24**, 6125 (2012).
45. C. Rao and B. Raveau: Transition metal oxides. *Annu. Rev. Phys. Chem.* **40**, 291 (1989).
46. Y. Tokura and N. Nagaosa: Orbital physics in transition-metal oxides. *Science* **288**, 462 (2000).
47. H. Bethe: Termaufspaltung in Kristallen. *Ann. Phys.* **395**, 133 (1929).
48. K. Van Benthem, C. Elsässer, and R. French: Bulk electronic structure of SrTiO<sub>3</sub>: Experiment and theory. *J. Appl. Phys.* **90**, 6156 (2001).
49. S. Saha, T. Sinha, and A. Mookerjee: Structural and optical properties of paraelectric SrTiO<sub>3</sub>. *J. Phys.: Condens. Matter* **12**, 3325 (2000).
50. W. Wunderlich, H. Ohta, and K. Koumoto: Enhanced effective mass in doped SrTiO<sub>3</sub> and related perovskites. *Phys. B* **404**, 2202 (2009).
51. O.N. Tufte and P.W. Chapman: Electron mobility in semi-conducting Strontium titanate. *Phys. Rev.* **155**, 796 (1967).
52. H. Frederikse, W.R. Thurber, and W.R. Hosler: Electronic transport in Strontium titanate. *Phys. Rev.* **134**, A442 (1964).
53. H. Frederikse and W.R. Hosler: Hall mobility in SrTiO<sub>3</sub>. *Phys. Rev.* **161**, 822 (1967).
54. A. Verma, A.P. Kajdos, T.A. Cain, S. Stemmer, and D. Jena: Intrinsic mobility limiting mechanisms in Lanthanum-doped strontium titanate. *Phys. Rev. Lett.* **112**, 216601 (2014).
55. E. Mikheev, B. Himmetoglu, A.P. Kajdos, P. Moetakef, T.A. Cain, C.G. Van De Walle, and S. Stemmer: Limitations to the room temperature mobility of two- and three-dimensional electron liquids in SrTiO<sub>3</sub>. *Appl. Phys. Lett.* **106**, 062102 (2015).
56. S.V. Ovsyannikov, V.V. Shchennikov, G.V. Vorontsov, A.Y. Manakov, A.Y. Likhacheva, and V.A. Kulbachinskii: Giant improvement of thermoelectric power factor of Bi<sub>2</sub>Te<sub>3</sub> under pressure. *J. Appl. Phys.* **104**, 053713 (2008).
57. S. Lee, G. Yang, R. Wilke, S. Trolier-Mckinstry, and C. Randall: Thermopower in highly reduced N-type ferroelectric and related perovskite oxides and the role of heterogeneous nonstoichiometry. *Phys. Rev. B: Condens. Matter Mater. Phys.* **79**, 134110 (2009).
58. S. Lee, R.H.T. Wilke, S. Trolier-Mckinstry, S. Zhang, and C.A. Randall: Sr<sub>x</sub>Ba<sub>1-x</sub>Nb<sub>2</sub>O<sub>6-δ</sub> ferroelectric-thermoelectrics: Crystal anisotropy, conduction mechanism, and power factor. *Appl. Phys. Lett.* **96**, 031910 (2010).
59. M. Yasukawa and N. Murayama: High-temperature thermoelectric properties of the oxide material: Ba<sub>1-x</sub>Sr<sub>x</sub>PbO<sub>3</sub> (x = 0–0.6). *J. Mater. Sci. Lett.* **16**, 1731 (1997).
60. M. Yasukawa and N. Murayama: A promising oxide material for high-temperature thermoelectric energy conversion: Ba<sub>1-x</sub>Sr<sub>x</sub>PbO<sub>3</sub> solid solution system. *Mater. Sci. Eng., B* **54**, 64 (1998).
61. M. Imada, A. Fujimori, and Y. Tokura: Metal-insulator transitions. *Rev. Mod. Phys.* **70**, 1039 (1998).
62. J. Zaanen, G.A. Sawatzky, and J.W. Allen: Band gaps and electronic structure of transition-metal compounds. *Phys. Rev. Lett.* **55**, 418 (1985).
63. G. Beni: Thermoelectric power of the narrow-band Hubbard chain at arbitrary electron density: Atomic limit. *Phys. Rev. B: Condens. Matter Mater. Phys.* **10**, 2186 (1974).
64. S. Mukerjee: Thermopower of the Hubbard model: Effects of multiple orbitals and magnetic fields in the atomic limit. *Phys. Rev. B: Condens. Matter Mater. Phys.* **72**, 195109 (2005).
65. P.M. Chaikin and G. Beni: Thermopower in the correlated hopping regime. *Phys. Rev. B: Condens. Matter Mater. Phys.* **13**, 647 (1976).
66. M. Ohtaki, H. Koga, T. Tokunaga, K. Eguchi, and H. Arai: Electrical transport properties and high-temperature thermoelectric performance of (Ca<sub>0.9</sub>M<sub>0.1</sub>)MnO<sub>3</sub> (M = Y, La, Ce, Sm, In, Sn, Sb, Pb, Bi). *J. Solid State Chem.* **120**, 105 (1995).
67. Y. Wang, Y. Sui, and W. Su: High temperature thermoelectric characteristics of Ca<sub>0.9</sub>R<sub>0.1</sub>MnO<sub>3</sub> (R = La, Pr, ..., Yb). *J. Appl. Phys.* **104**, 093703 (2008).
68. S. Hébert, C. Martin, A. Maignan, R. Frésard, J. Hejtmanek, and B. Raveau: Large thermopower in metallic oxides: Misfit cobaltites and mangano-ruthenates. *Arch., Condens. Matter*, arXiv preprint 0110270 (2001).
69. W.J. Weber, C.W. Griffin, and J.L. Bates: Effects of cation substitution on electrical and thermal transport properties of YCrO<sub>3</sub> and LaCrO<sub>3</sub>. *J. Am. Ceram. Soc.* **70**, 265 (1987).
70. S. Hébert, Y. Klein, A. Maignan, J. Hejtmanek, and B. Dabrowski: Thermopower of ruthenium metallic oxides: Large influence of the spin degeneracy term. *Proceedings of 25th International Conference on thermoelectrics, 2006*, Vol. **318**, ICT '06, 2006.
71. R. Funahashi, I. Matsubara, H. Ikuta, T. Takeuchi, U. Mizutani, and S. Sodeoka: An oxide single crystal with high thermoelectric performance in air. *Jpn. J. Appl. Phys.* **39**(2), 1127 (2000).
72. I. Terasaki: Cobalt oxides, and Kondo semiconductors: A pseudogap system as a thermoelectric material. *Mater. Trans.* **42**, 951 (2001).
73. M. Lee, L. Viciu, L. Li, Y. Wang, M. Foo, S. Watauchi, R. Pascal, R. Cava, and N. Ong: Large enhancement of the thermopower in Na<sub>x</sub>CoO<sub>2</sub> at high Na doping. *Nat. Mater.* **5**, 537 (2006).
74. S. Hébert, D. Berthebaud, R. Daou, Y. Bréard, D. Pelloquin, E. Guilmeau, F. Gascoin, O. Lebedev, and A. Maignan: Searching for new thermoelectric materials: Some examples among oxides, sulfides and selenides. *J. Phys.: Condens. Matter* **28**, 013001 (2015).

75. J.R. Sootsman, D-Y. Chung, and M.G. Kanatzidis: New and old concepts in thermoelectric materials. *Angew. Chem., Int. Ed.* **48**, 8616 (2009).
76. Y. Wang, N. Rogado, R. Cava, and N. Ong: Spin entropy as the likely source of enhanced thermopower in  $\text{Na}_x\text{Co}_2\text{O}_4$ . *Nature* **423**, 425 (2003).
77. J.B. Goodenough: An interpretation of the magnetic properties of the perovskite-type mixed crystals  $\text{La}_{1-x}\text{Sr}_x\text{CoO}_{3-\delta}$ . *J. Phys. Chem. Solids* **6**, 287 (1958).
78. I. Terasaki, H. Tanaka, A. Satake, S. Okada, and T. Fujii: Out-of-plane thermal conductivity of the layered thermoelectric oxide  $\text{Bi}_{2-x}\text{Pb}_x\text{Sr}_2\text{Co}_2\text{O}_y$ . *Phys. Rev. B: Condens. Matter Mater. Phys.* **70**, 214106 (2004).
79. T. Fujii and I. Terasaki: Block-layer concept for the layered cobalt oxide: A design for thermoelectric oxides. In *Chemistry, Physics, and Materials Science of Thermoelectric Materials*, M.G. Kanatzidis, S.D. Mahanti, and T.P. Hogan, eds. (Springer, Boston, 2003); pp. 71–87.
80. D.G. Schlom, J.N. Eckstein, E.S. Hellman, S.K. Streiffer, J.S. Harris, M.R. Beasley, J.C. Bravman, T.H. Geballe, C. Webb, K.E. Von Dessenbeck, and F. Turner: Molecular beam epitaxy of layered Dy–Ba–Cu–O compounds. *Appl. Phys. Lett.* **53**, 1660 (1988).
81. J. Kwo, M. Hong, D.J. Trevor, R.M. Fleming, A.E. White, R.C. Farrow, A.R. Kortan, and K.T. Short: In situ epitaxial growth of  $\text{Y}_1\text{Ba}_2\text{Cu}_3\text{O}_{7-x}$  films by molecular beam epitaxy with an activated oxygen source. *Appl. Phys. Lett.* **53**, 2683 (1988).
82. R.J. Spah, H.F. Hess, H.L. Stormer, A.E. White, and K.T. Short: Parameters for in situ growth of high  $T_c$  superconducting thin films using an oxygen plasma source. *Appl. Phys. Lett.* **53**, 441 (1988).
83. J.N. Eckstein and I. Bozovic: High-temperature superconducting multilayers and heterostructures grown by atomic layer-by-layer molecular beam epitaxy. *Annu. Rev. Mater. Sci.* **25**, 679 (1995).
84. D. Dijkkamp, T. Venkatesan, X.D. Wu, S.A. Shaheen, N. Jisrawi, Y.H. Min-Lee, W.L. McLean, and M. Croft: Preparation of Y–Ba–Cu oxide superconductor thin films using pulsed laser evaporation from high  $T_c$  bulk material. *Appl. Phys. Lett.* **51**, 619 (1987).
85. R. Ramesh, K. Luther, B. Wilkens, D.L. Hart, E. Wang, J.M. Tarascon, A. Inam, X.D. Wu, and T. Venkatesan: Epitaxial growth of ferroelectric bismuth titanate thin films by pulsed laser deposition. *Appl. Phys. Lett.* **57**, 1505 (1990).
86. G. Rijnders, G. Koster, V. Leca, D.H.A. Blank, and H. Rogalla: Imposed layer-by-layer growth with pulsed laser interval deposition. *Appl. Surf. Sci.* **168**, 223 (2000).
87. U. Poppe, J. Schubert, R.R. Arons, W. Evers, C.H. Freiburg, W. Reichert, K. Schmidt, W. Sybertz, and K. Urban: Direct production of crystalline superconducting thin films of  $\text{YBa}_2\text{Cu}_3\text{O}_7$  by high-pressure oxygen sputtering. *Solid State Commun.* **66**, 661 (1988).
88. H. Koinuma, M. Kawasaki, M. Funabashi, T. Hasegawa, K. Kishio, K. Kitazawa, K. Fueki, and S. Nagata: Preparation of superconducting thin films of  $(\text{La}_{1-x}\text{Sr}_x)_y\text{CuO}_{4-\delta}$  by sputtering. *J. Appl. Phys.* **62**, 1524 (1987).
89. B. Pachaly, R. Bruchhaus, D. Pitzer, H. Huber, W. Wersing, and F. Koch: Pyroelectric properties of lead titanate thin films deposited on Pt-coated Si wafers by multi-target sputtering. *Integr. Ferroelectr.* **5**, 333 (1994).
90. C.B. Eom, J.Z. Sun, K. Yamamoto, A.F. Marshall, K.E. Luther, T.H. Geballe, and S.S. Laderman: In situ grown  $\text{YBa}_2\text{Cu}_3\text{O}_{7-\delta}$  thin films from single-target magnetron sputtering. *Appl. Phys. Lett.* **55**, 595 (1989).
91. C.H. Ahn, J-M. Triscone, N. Archibald, M. Decroux, R.H. Hammond, T.H. Geballe, O. Fischer, and M.R. Beasley: Ferroelectric field effect in epitaxial thin film oxide  $\text{SrCuO}_2/\text{Pb}(\text{Zr}_{0.52}\text{Ti}_{0.48})\text{O}_3$  heterostructures. *Science* **269**, 373 (1995).
92. X.X. Xi, G. Linker, O. Meyer, E. Nold, B. Obst, F. Ratzel, R. Smithey, B. Strehlau, F. Weschenfelder, and J. Geerk: Superconducting and structural properties of  $\text{YBaCuO}$  thin films deposited by inverted cylindrical magnetron sputtering. *Z. Phys. B: Condens. Matter* **74**, 13 (1989).
93. R.L. Sandstrom, W.J. Gallagher, T.R. Dinger, R.H. Koch, R.B. Laibowitz, A.W. Kleinsasser, R.J. Gambino, B. Bumble, and M.F. Chisholm: Reliable single-target sputtering process for high-temperature superconducting films and devices. *Appl. Phys. Lett.* **53**, 444 (1988).
94. G.R. Bai, I-F. Tsu, A. Wang, C.M. Foster, C.E. Murray, and V.P. Dravid: In situ growth of highly oriented  $\text{Pb}(\text{Zr}_{0.5}\text{Ti}_{0.5})\text{O}_3$  thin films by low-temperature metal–organic chemical vapor deposition. *Appl. Phys. Lett.* **72**, 1572 (1998).
95. M. De Keijsers and G. Dormans: Chemical vapor deposition of electroceramic thin films. *MRS Bull.* **21**, 37 (1996).
96. M.V.R. Murty, S.K. Streiffer, G.B. Stephenson, J.A. Eastman, G.R. Bai, A. Munkholm, O. Auciello, and C. Thompson: In situ x-ray scattering study of  $\text{PbTiO}_3$  chemical-vapor deposition. *Appl. Phys. Lett.* **80**, 1809 (2002).
97. M. Okada, S. Takai, M. Amemiya, and K. Tominaga: Preparation of *c*-axis-oriented  $\text{PbTiO}_3$  thin films by MOCVD under reduced pressure. *Jpn. J. Appl. Phys.* **28**, 1030 (1989).
98. B.S. Kwak, E.P. Boyd, and A. Erbil: Metal organic chemical vapor deposition of  $\text{PbTiO}_3$  thin films. *Appl. Phys. Lett.* **53**, 1702 (1988).
99. R.W. Schwartz: Chemical solution deposition of perovskite thin films. *Chem. Mater.* **9**, 2325 (1997).
100. S. Ohta, T. Nomura, H. Ohta, M. Hirano, H. Hosono, and K. Koumoto: Large thermoelectric performance of heavily Nb-doped  $\text{SrTiO}_3$  epitaxial film at high temperature. *Appl. Phys. Lett.* **87**, 092108 (2005).
101. J. Ravichandran, W. Siemons, D-W. Oh, J.T. Kardel, A. Chari, H. Heijmerikx, M.L. Scullin, A. Majumdar, R. Ramesh, and D.G. Cahill: High-temperature thermoelectric response of double-doped  $\text{SrTiO}_3$  epitaxial films. *Phys. Rev. B: Condens. Matter Mater. Phys.* **82**, 165126 (2010).
102. S. Ohta, T. Nomura, H. Ohta, and K. Koumoto: High-temperature carrier transport and thermoelectric properties of heavily La- or Nb-doped  $\text{SrTiO}_3$  single crystals. *J. Appl. Phys.* **97**, 034106 (2005).
103. T. Bak, J. Nowotny, C.C. Sorrell, M.F. Zhou, and E.R. Vance: Charge transport in  $\text{CaTiO}_3$ : II. Thermoelectric power. *J. Mater. Sci.: Mater. Electron.* **15**, 645 (2004).
104. T. Bak, T. Burg, J. Nowotny, and P.J. Blennerhassett: Electrical conductivity and thermoelectric power of  $\text{CaTiO}_3$  at n–p transition. *Adv. Appl. Ceram.* **106**, 101 (2013).
105. B.G. Brahmecha: Thermoelectric effect in semiconducting barium titanate. *Jpn. J. Appl. Phys.* **8**, 883 (1969).
106. M. Nasir Khan, H-T. Kim, H. Minami, and H. Uwe: Thermoelectric properties of niobium doped hexagonal barium titanate. *Mater. Lett.* **47**, 95 (2001).
107. T. Kolodiazny, A. Petric, M. Niewczas, C. Bridges, A. Safa-Sefat, and J.E. Greedan: Thermoelectric power, Hall effect, and mobility of n-type  $\text{BaTiO}_3$ . *Phys. Rev. B: Condens. Matter Mater. Phys.* **68**, 085205 (2003).
108. H. Ohta, S. Kim, Y. Mune, T. Mizoguchi, K. Nomura, S. Ohta, T. Nomura, Y. Nakanishi, Y. Ikuhara, M. Hirano, H. Hosono, and K. Koumoto: Giant thermoelectric Seebeck coefficient of two-dimensional electron gas in  $\text{SrTiO}_3$ . *Nat. Mater.* **6**, 129 (2007).
109. H. Ohta, Y. Mune, K. Koumoto, T. Mizoguchi, and Y. Ikuhara: Critical thickness for giant thermoelectric Seebeck coefficient of

- 2DEG confined in SrTiO<sub>3</sub>/SrTi<sub>0.8</sub>Nb<sub>0.2</sub>O<sub>3</sub> superlattices. *Thin Solid Films* **516**, 5916 (2008).
110. H. Ohta, R. Huang, and Y. Ikuhara: Large enhancement of the thermoelectric Seebeck coefficient for amorphous oxide semiconductor superlattices with extremely thin conductive layers. *Phys. Status Solidi RRL* **2**, 105 (2008).
  111. J. Ravichandran, A.K. Yadav, R. Cheaito, P.B. Rossen, A. Soukiassian, S.J. Suresha, J.C. Duda, B.M. Foley, C-H. Lee, Y. Zhu, A.W. Lichtenberger, J.E. Moore, D.A. Muller, D.G. Schlom, P.E. Hopkins, A. Majumdar, R. Ramesh, and M.A. Zurbuchen: Crossover from incoherent to coherent phonon scattering in epitaxial oxide superlattices. *Nat. Mater.* **13**, 168 (2014).
  112. A.I. Abutaha, S.R.S. Kumar, K. Li, A.M. Dehkordi, T.M. Tritt, and H.N. Alshareef: Enhanced thermoelectric figure-of-merit in thermally robust, nanostructured superlattices based on SrTiO<sub>3</sub>. *Chem. Mater.* **27**, 2165 (2015).
  113. K. Kerman, S. Ramanathan, J.D. Baniecki, M. Ishii, Y. Kotaka, H. Aso, K. Kurihara, R. Schafrank, and A. Vailionis: Thermopower in quantum confined La-doped SrTiO<sub>3</sub> epitaxial heterostructures. *Appl. Phys. Lett.* **103**, 173904 (2013).
  114. A.I. Abutaha, S.R. Sarath Kumar, A. Mehdizadeh Dehkordi, T.M. Tritt, and H.N. Alshareef: Doping site dependent thermoelectric properties of epitaxial Strontium titanate thin films. *J. Mater. Chem. C* **2**, 9712 (2014).
  115. S.R.S. Kumar, A.Z. Barasheed, and H.N. Alshareef: High temperature thermoelectric properties of strontium titanate thin films with oxygen vacancy and niobium doping. *ACS Appl. Mater. Interfaces* **5**, 7268 (2013).
  116. K.H. Lee, A. Ishizaki, S.W. Kim, H. Ohta, and K. Koumoto: Preparation and thermoelectric properties of heavily Nb-doped SrO(SrTiO<sub>3</sub>)<sub>1</sub> epitaxial films. *J. Appl. Phys.* **102**, 033702 (2007).
  117. M. Yamamoto, H. Ohta, and K. Koumoto: Thermoelectric phase diagram in a CaTiO<sub>3</sub>-SrTiO<sub>3</sub>-BaTiO<sub>3</sub> system. *Appl. Phys. Lett.* **90**, 072101 (2007).
  118. J.D. Baniecki, M. Ishii, H. Aso, K. Kobayashi, K. Kurihara, K. Yamanaka, A. Vailionis, and R. Schafrank: Electronic transport behavior of off-stoichiometric La and Nb doped Sr<sub>x</sub>Ti<sub>3-x</sub>O<sub>3-δ</sub> epitaxial thin films and donor doped single-crystalline SrTiO<sub>3</sub>. *Appl. Phys. Lett.* **99**, 232111 (2011).
  119. B. Jalan and S. Stemmer: Large Seebeck coefficients and thermoelectric power factor of La-doped SrTiO<sub>3</sub> thin films. *Appl. Phys. Lett.* **97**, 042106 (2010).
  120. T.A. Cain, A.P. Kajdos, and S. Stemmer: La-doped SrTiO<sub>3</sub> films with large cryogenic thermoelectric power factors. *Appl. Phys. Lett.* **102**, 182101 (2013).
  121. D-W. Oh, J. Ravichandran, C-W. Liang, W. Siemons, B. Jalan, C.M. Brooks, M. Huijben, D.G. Schlom, S. Stemmer, L.W. Martin, A. Majumdar, R. Ramesh, and D.G. Cahill: Thermal conductivity as a metric for the crystalline quality of SrTiO<sub>3</sub> epitaxial layers. *Appl. Phys. Lett.* **98**, 221904 (2011).
  122. S. Wiedigen, T. Kramer, M. Feuchter, I. Knorr, N. Nee, J. Hoffmann, M. Kamlah, C.A. Volkert, and C. Jooss: Interplay of point defects, biaxial strain, and thermal conductivity in homoepitaxial SrTiO<sub>3</sub> thin films. *Appl. Phys. Lett.* **100**, 061904 (2012).
  123. D.G. Schlom, L.Q. Chen, X. Pan, A. Schmehl, and M.A. Zurbuchen: A thin film approach to engineering functionality into oxides. *J. Am. Ceram. Soc.* **91**, 2429 (2008).
  124. C.M. Brooks, L.F. Kourkoutis, T. Heeg, J. Schubert, D.A. Muller, and D.G. Schlom: Growth of homoepitaxial SrTiO<sub>3</sub> thin films by molecular-beam epitaxy. *Appl. Phys. Lett.* **94**, 162905 (2009).
  125. E. Breckenfeld, R. Wilson, J. Karthik, A.R. Damodaran, D.G. Cahill, and L.W. Martin: Effect of growth induced (non) stoichiometry on the structure, dielectric response, and thermal conductivity of SrTiO<sub>3</sub> thin films. *Chem. Mater.* **24**, 331 (2012).
  126. W.S. Choi, H.K. Yoo, and H. Ohta: Polaron transport and thermoelectric behavior in La-doped SrTiO<sub>3</sub> thin films with elemental vacancies. *Adv. Funct. Mater.* **25**, 799 (2015).
  127. J. Robertson and S.J. Clark: Limits to doping in oxides. *Phys. Rev. B: Condens. Matter Mater. Phys.* **83**, 075205 (2011).
  128. E. Ertekin, V. Srinivasan, J. Ravichandran, P.B. Rossen, W. Siemons, A. Majumdar, R. Ramesh, and J.C. Grossman: Interplay between intrinsic defects, doping, and free carrier concentration in SrTiO<sub>3</sub> thin films. *Phys. Rev. B: Condens. Matter Mater. Phys.* **85**, 195460 (2012).
  129. A. Janotti, B. Jalan, S. Stemmer, and C.G. Van De Walle: Effects of doping on the lattice parameter of SrTiO<sub>3</sub>. *Appl. Phys. Lett.* **100**, 262104 (2012).
  130. A. Janotti, J.B. Varley, M. Choi, and C.G. Van De Walle: Vacancies and small Polarons in SrTiO<sub>3</sub>. *Phys. Rev. B: Condens. Matter Mater. Phys.* **90**, 085202 (2014).
  131. S.R. Sarath Kumar, A.I. Abutaha, M.N. Hedhili, and H.N. Alshareef: Modeling the transport properties of epitaxially grown thermoelectric oxide thin films using spectroscopic ellipsometry. *Appl. Phys. Lett.* **100**, 052110 (2012).
  132. Y. Krockenberger, I. Fritsch, G. Cristiani, A. Matveev, L. Alff, H-U. Habermeier, and B. Keimer: Epitaxial growth of Na<sub>x</sub>CoO<sub>2</sub> thin films by pulsed-laser deposition. *Appl. Phys. Lett.* **86**, 191913 (2005).
  133. L. Yu, L. Gu, Y. Wang, P.X. Zhang, and H-U. Habermeier: Epitaxial layered cobaltite Na<sub>x</sub>CoO<sub>2</sub> thin films grown on planar and vicinal cut substrates. *J. Cryst. Growth* **328**, 34 (2011).
  134. A. Venimadhav, Z. Ma, Q. Li, A. Soukiassian, X. Xi, D. Schlom, R. Arroyave, Z. Liu, M. Lee, and N. Ong: Thermoelectric properties of epitaxial and topotaxial Na<sub>x</sub>CoO<sub>2</sub> thin films. *Mater. Res. Soc. Symp. Proc.* **886**, 0886 (2006).
  135. P. Brinks, H. Heijmerikx, T.A. Hendriks, G. Rijnders, and M. Huijben: Achieving chemical stability in thermoelectric Na<sub>x</sub>CoO<sub>2</sub> thin films. *RSC Adv.* **2**, 6023 (2012).
  136. P. Brinks, B. Kuiper, E. Breckenfeld, G. Koster, L.W. Martin, G. Rijnders, and M. Huijben: Enhanced thermoelectric power factor of Na<sub>x</sub>CoO<sub>2</sub> thin films by structural engineering. *Adv. Energy Mater.* **4**, 1301927 (2014).
  137. J.Y. Son, B.G. Kim, and J.H. Cho: Kinetically controlled thin-film growth of layered β- and γ-Na<sub>x</sub>CoO<sub>2</sub> cobaltate. *Appl. Phys. Lett.* **86**, 221918 (2005).
  138. X.P. Zhang, Y.S. Xiao, H. Zhou, B.T. Xie, C.X. Yang, and Y.G. Zhao: Surface morphology, structure and transport property of Na<sub>x</sub>CoO<sub>2</sub> thin films grown by pulsed laser deposition. *Mater. Sci. Forum* **475-479**, 3807 (2005).
  139. J. Buršík, M. Soroka, K. Knížek, J. Hirschner, P. Levinský, and J. Hejtmánek: Oriented thin films of Na<sub>0.6</sub>CoO<sub>2</sub> and Ca<sub>3</sub>Co<sub>4</sub>O<sub>9</sub> deposited by spin-coating method on polycrystalline substrate. *Thin Solid Films* **603**, 400 (2016).
  140. A. Venimadhav, A. Soukiassian, D.A. Tenne, Q. Li, X.X. Xi, D.G. Schlom, R. Arroyave, Z.K. Liu, H.P. Sun, X. Pan, M. Lee, and N.P. Ong: Structural and transport properties of epitaxial Na<sub>x</sub>CoO<sub>2</sub> thin films. *Appl. Phys. Lett.* **87**, 172104 (2005).
  141. S. Wang, A. Venimadhav, S. Guo, K. Chen, Q. Li, A. Soukiassian, D.G. Schlom, M.B. Katz, X.Q. Pan, W. Wong-Ng, M.D. Vaudin, and X.X. Xi: Structural and thermoelectric properties of Bi<sub>2</sub>Sr<sub>2</sub>Co<sub>2</sub>O<sub>y</sub> thin films on LaAlO<sub>3</sub> (100) and fused silica substrates. *Appl. Phys. Lett.* **94**, 022110 (2009).
  142. S. Wang, S. Chen, G. Yan, F. Liu, S. Dai, J. Wang, W. Yu, and G. Fu: Fabrication and thermoelectric properties of C-axis

- oriented nanocrystalline  $\text{Bi}_2\text{Sr}_2\text{Co}_2\text{O}_y$  thin films. *Thin Solid Films* **534**, 168 (2013).
143. J. Ravichandran, A.K. Yadav, W. Siemons, M.A. McGuire, V. Wu, A. Vailionis, A. Majumdar, and R. Ramesh: Size effects on thermoelectricity in a strongly correlated oxide. *Phys. Rev. B: Condens. Matter Mater. Phys.* **85**, 085112 (2012).
  144. B. Rivas-Murias, J. Manuel Vila-Fungueiriño, and F. Rivadulla: High quality thin films of thermoelectric misfit cobalt oxides prepared by a chemical solution method. *Sci. Rep.* **5**, 11889 (2015).
  145. I. Tsukada, I. Terasaki, T. Hoshi, F. Yura, and K. Uchinokura: Thin film growth of layered cobalt-oxide  $\text{Bi}_2\text{Sr}_3\text{Co}_2\text{O}_{9+\delta}$  nearly isomorphic to  $\text{Bi}_2\text{Sr}_2\text{CaCu}_2\text{O}_{8+\delta}$  superconductors. *J. Appl. Phys.* **76**, 1317 (1994).
  146. A. Sakai, T. Kanno, S. Yotsuhashi, S. Okada, and H. Adachi: Preparation of metastable  $\text{Sr}_3\text{Co}_4\text{O}_9$  epitaxial thin films with controlled orientation and their anisotropic thermoelectric properties. *J. Appl. Phys.* **99**, 093704 (2006).
  147. T. Kanno, S. Yotsuhashi, and H. Adachi: Anisotropic thermoelectric properties in layered cobaltite  $\text{A}_x\text{CoO}_2$  (A = Sr and Ca) thin films. *Appl. Phys. Lett.* **85**, 739 (2004).
  148. G. Yan, Z. Bai, S. Wang, L. Sun, J. Wang, and G. Fu: Dependence of oxygen content on transverse thermoelectric effect in tilted  $\text{Bi}_2\text{Sr}_2\text{Co}_2\text{O}_y$  thin films. *Appl. Opt.* **53**, 4211 (2014).
  149. W. Shu-Fang, Y. Guo-Ying, C. Shan-Shan, B. Zi-Long, W. Jiang-Long, Y. Wei, and F. Guang-Sheng: Effect of microstructure on the thermoelectric properties of CSD-grown  $\text{Bi}_2\text{Sr}_2\text{Co}_2\text{O}_y$  thin films. *Chin. Phys. B* **22**, 037302 (2013).
  150. X. Zhu, D. Shi, S. Dou, Y. Sun, Q. Li, L. Wang, W. Li, W. Yeoh, R. Zheng, and Z. Chen: (001)-oriented  $\text{Bi}_2\text{Sr}_2\text{Co}_2\text{O}_y$  and  $\text{Ca}_3\text{Co}_4\text{O}_9$  films: Self-assembly orientation and growth mechanism by chemical solution deposition. *Acta Mater.* **58**, 4281 (2010).
  151. A. Weidenkaff, R. Robert, M. Aguirre, L. Bocher, T. Lippert, and S. Canulescu: Development of thermoelectric oxides for renewable energy conversion technologies. *Renewable Energy* **33**, 342 (2008).
  152. D.S. Alfaruq, E.H. Otal, M.H. Aguirre, S. Populoh, and A. Weidenkaff: Thermoelectric properties of  $\text{CaMnO}_3$  films obtained by soft chemistry synthesis. *J. Mater. Res.* **27**, 985 (2012).
  153. P. Jha, T.D. Sands, L. Cassels, P. Jackson, T. Favaloro, B. Kirk, J. Zide, X. Xu, and A. Shakouri: Cross-plane electronic and thermal transport properties of p-type  $\text{La}_{0.67}\text{Sr}_{0.33}\text{MnO}_3/\text{LaMnO}_3$  perovskite oxide metal/semiconductor superlattices. *J. Appl. Phys.* **112**, 063714 (2012).
  154. P. Jha, T.D. Sands, P. Jackson, C. Bomberger, T. Favaloro, S. Hodson, J. Zide, X. Xu, and A. Shakouri: Cross-plane thermoelectric transport in p-type  $\text{La}_{0.67}\text{Sr}_{0.33}\text{MnO}_3/\text{LaMnO}_3$  oxide metal/semiconductor superlattices. *J. Appl. Phys.* **113**, 193702 (2013).
  155. A.N. Banerjee, R. Maity, P.K. Ghosh, and K.K. Chattopadhyay: Thermoelectric properties and electrical characteristics of sputter-deposited p-CuAlO<sub>2</sub> thin films. *Thin Solid Films* **474**, 261 (2005).
  156. R. Robert, M.H. Aguirre, L. Bocher, M. Trottmann, S. Heiroth, T. Lippert, M. Döbeli, and A. Weidenkaff: Thermoelectric properties of  $\text{LaCo}_{1-x}\text{Ni}_x\text{O}_3$  polycrystalline samples and epitaxial thin films. *Solid State Sci.* **10**, 502 (2008).
  157. D.G. Cahill: Analysis of heat flow in layered structures for time-domain thermoreflectance. *Rev. Sci. Instrum.* **75**, 5119 (2004).
  158. D.G. Cahill: Thermal conductivity measurement from 30 to 750 K: The  $3\omega$  method. *Rev. Sci. Instrum.* **61**, 802 (1990).
  159. D.G. Cahill, W.K. Ford, K.E. Goodson, G.D. Mahan, A. Majumdar, H.J. Maris, R. Merlin, and S.R. Phillpot: Nanoscale thermal transport. *J. Appl. Phys.* **93**, 793 (2002).
  160. D.G. Cahill, P.V. Braun, G. Chen, D.R. Clarke, S. Fan, K.E. Goodson, P. Keblinski, W.P. King, G.D. Mahan, A. Majumdar, H.J. Maris, S.R. Phillpot, E. Pop, and L. Shi: Nanoscale thermal transport. II. 2003–2012. *Appl. Phys. Rev.* **1**, 011305 (2014).
  161. J. Ravichandran, J.T. Kardel, M.L. Scullin, J.H. Bahk, H. Heijmerikx, J.E. Bowers, and A. Majumdar: An apparatus for simultaneous measurement of electrical conductivity and thermopower of thin films in the temperature range of 300–750 K. *Rev. Sci. Instrum.* **82**, 015108 (2011).
  162. A.T. Burkov, A. Heinrich, P.P. Konstantinov, T. Nakama, and K. Yagasaki: Experimental set-up for thermopower and resistivity measurements at 100–1300 K. *Meas. Sci. Technol.* **12**, 264 (2001).
  163. O. Boffoué, A. Jacquot, A. Dauscher, B. Lenoir, and M. Stölzer: Experimental setup for the measurement of the electrical resistivity and thermopower of thin films and bulk materials. *Rev. Sci. Instrum.* **76**, 053907 (2005).
  164. J. Ravichandran, W. Siemons, M.L. Scullin, S. Mukerjee, M. Huijben, J.E. Moore, A. Majumdar, and R. Ramesh: Tuning the electronic effective mass in double-doped  $\text{SrTiO}_3$ . *Phys. Rev. B: Condens. Matter Mater. Phys.* **83**, 035101 (2011).
  165. J. Ravichandran, W. Siemons, H. Heijmerikx, M. Huijben, A. Majumdar, and R. Ramesh: An epitaxial transparent conducting perovskite oxide: Double-Doped  $\text{SrTiO}_3$ . *Chem. Mater.* **22**, 3983 (2010).
  166. K. Sugiura, H. Ohta, and K. Koumoto: Thermoelectric performance of epitaxial thin films of layered cobalt oxides grown by reactive solid-phase epitaxy with topotactic ion-exchange methods. *Int. J. Appl. Ceram. Technol.* **4**, 308 (2007).
  167. C. Yu, M.L. Scullin, M. Huijben, R. Ramesh, and A. Majumdar: Thermal conductivity reduction in oxygen-deficient strontium titanates. *Appl. Phys. Lett.* **92**, 191911 (2008).
  168. C.M. Brooks, R.B. Wilson, A. Schäfer, J.A. Mundy, M.E. Holtz, D.A. Muller, J. Schubert, D.G. Cahill, and D.G. Schlom: Tuning thermal conductivity in Homoepitaxial  $\text{SrTiO}_3$  films via defects. *Appl. Phys. Lett.* **107**, 051902 (2015).
  169. B.M. Foley, H.J. Brown-Shaklee, J.C. Duda, R. Cheaito, B.J. Gibbons, D. Medlin, J.F. Ihlefeld, and P.E. Hopkins: Thermal conductivity of nano-grained  $\text{SrTiO}_3$  thin films. *Appl. Phys. Lett.* **101**, 231908 (2012).
  170. Y. Mune, H. Ohta, K. Koumoto, T. Mizoguchi, and Y. Ikuhara: Enhanced Seebeck coefficient of quantum-confined electrons in  $\text{SrTiO}_3/\text{SrTi}_{0.8}\text{Nb}_{0.2}\text{O}_3$  superlattices. *Appl. Phys. Lett.* **91**, 192105 (2007).
  171. W.S. Choi, H. Ohta, and H.N. Lee: Thermopower enhancement by fractional layer control in 2D oxide superlattices. *Adv. Mater.* **26**, 6701 (2014).
  172. A. Ohtomo and H. Hwang: A high-mobility electron gas at the  $\text{LaAlO}_3/\text{SrTiO}_3$  heterointerface. *Nature* **427**, 423 (2004).
  173. I. Pallecchi, M. Codda, E. Galleani d'Agliano, D. Marré, A.D. Caviglia, N. Reyren, S. Gariglio, and J-M. Triscone: Seebeck effect in the conducting  $\text{LaAlO}_3/\text{SrTiO}_3$  interface. *Phys. Rev. B: Condens. Matter Mater. Phys.* **81**, 085414 (2010).
  174. A. Jost, V.K. Guduru, S. Wiedmann, J.C. Maan, U. Zeitler, S. Wenderich, A. Brinkman, and H. Hilgenkamp: Transport and thermoelectric properties of the  $\text{LaAlO}_3/\text{SrTiO}_3$  interface.

- Phys. Rev. B: Condens. Matter Mater. Phys.* **91**, 045304 (2015).
175. I. Pallecchi, F. Telesio, D. Li, A. Fête, S. Gariglio, J-M. Triscone, A. Filippetti, P. Delugas, V. Fiorentini, and D. Marré: Giant oscillating thermopower at oxide interfaces. *Nature Commun.* **6**, 6678 (2015).
176. I. Pallecchi, F. Telesio, D. Marré, D. Li, S. Gariglio, J-M. Triscone, and A. Filippetti: Large phonon-drag enhancement induced by narrow quantum confinement at the LaAlO<sub>3</sub>/SrTiO<sub>3</sub> interface. *Phys. Rev. B: Condens. Matter Mater. Phys.* **93**, 195309 (2016).
177. T.A. Cain, S. Lee, P. Moetakef, L. Balents, S. Stemmer, and S. James Allen: Seebeck coefficient of a quantum confined, high-electron-density electron gas in SrTiO<sub>3</sub>. *Appl. Phys. Lett.* **100**, 161601 (2012).
178. P. Brinks, G. Rijnders, and M. Huijben: Size effects on thermoelectric behavior of ultrathin Na<sub>x</sub>CoO<sub>2</sub> films. *Appl. Phys. Lett.* **105**, 193902 (2014).
179. M. Simkin and G. Mahan: Minimum thermal conductivity of superlattices. *Phys. Rev. Lett.* **84**, 927 (2000).
180. J.F. Schooley, W.R. Hosler, and M.L. Cohen: Superconductivity in semiconducting SrTiO<sub>3</sub>. *Phys. Rev. Lett.* **12**, 474 (1964).